AIMS Mathematics, 11(2): 4479–4521.
DOI: 10.3934/math.2026180
Received: 08 November 2025
Revised: 19 December 2025
Accepted: 09 January 2026
Published: 13 February 2026

http://www.aimspress.com/journal/Math

Research article

Mixed exponentially weighted moving average – double moving average control chart base on sign statistic and its applications

Weerawat Sudsutad, Yupaporn Areepong and Saowanit Sukparungsee*

Department of Applied Statistics, Faculty of Applied Science, King Mongkut's University of Technology North Bangkok, Bangkok, Thailand

* **Correspondence:** Email: saowanit.s@sci.kmutnb.ac.th.

Abstract: Control charts are proposed with the assumption that the process's quality parameter follows a normal distribution. However, in fact, the normality assumption is rarely applied in practice. Parametric charts have a greater false alarm rate and more incorrect out-of-control comparisons in non-normal scenarios. Because the actual distribution of the quality parameter at issue is unknown, nonparametric charts are a strong and useful tool for evaluating a technique. This work proposes a nonparametric mixed exponentially weighted moving average–double moving average chart based on sign statistics to monitor the change in the process's mean under symmetric and asymmetric distributions. The proposed techniques are notable for their efficiency in identifying modest and persistent shifts in the process's location that match the supplied smoothing parameter values. The efficacy of the proposed chart was established through Monte Carlo (MC) simulation utilizing an average run length (ARL), a median run length (MRL), and the standard deviation of run length (S-DRL). Additionally, the average extra quadratic loss (AEQL), performance comparison index (PCI), and relative mean index (RMI) are additional metrics of overall performance that are applied to assess the utility of control charts. The proposed chart is found to be more effective in detecting a small mean shift in the processes faster than alternative charts such as the Shewhart, exponentially weighted moving average (EWMA), moving average (MA), double moving average (DMA), mixed EMMA–MA (MEM), and mixed EWMA–DMA (MEDM) charts under different symmetrical and asymmetrical distributions. In addition, the proposed and existing charts have been applied to three real-life data-sets: (i) The die-casting hot chamber process used in manufacturing zinc alloy parts for the sanitary industry, (ii) the survival times of a cluster of patients suffering from head and neck cancer disease who were treated with radiotherapy, and (iii) the measurements of the outer diameter at the base of the stem of an exhaust valve bridge.

Keywords: nonparametric; control chart; exponentially weighted moving average; double moving average; sign; average run length
Mathematics Subject Classification: 62G05, 62P10, 62P30

1. Introduction

Improving product quality is an important goal of industries. An industry's favorable reputation in the worldwide market stems from its excellent product quality and consumer approval. Control charts are used to help industries manage high-quality products, which are an important tool in statistical process control (SPC). They have a process operating on two control limits: Upper and lower control limits (UCL/LCL). The process is considered to be out of control (OOC) if the quality feature is outside of these limits, whereas it is considered to be in control (IC) if it is. Process outputs are often influenced by unique causes of variance rather than conventional ones. Control charts assist us in detecting these particular causes of variation early on, therefore minimizing the cost effects. These properties are quite important for producing high-quality goods [1]. Each type of data may be represented by different control charts. Control charts are applied in various disciplines, including medical science [2, 3], chemistry [4], the packaging and manufacturing industries [5], aircraft industries [6, 7], and ecological and environmental sciences [8] (see also the references cited in the aforementioned works).

Certain essential assumptions, like normalcy and independence, are required by these charting schemes. However, these assumptions may not always hold in many real-world scenarios, such as evaluating semiconductor and chemical processes, quantifying cutting equipment wear procedures, and estimating the lifespan of accelerated life test samples. Control charts have proven to be a particularly useful tool within SPC, which was first introduced in 1920 by Shewhart [9]. It is only responsive to large changes in the process. While these control charts are simple to use and effective at detecting substantial process alterations, their dependence on the current sample's data limits their ability to detect minor shifts. To overcome these constraints, several researchers have attempted to construct memory-based control charts. Many control charts focus on previous data that were created. In 1954, Page [10] invented the cumulative sum (CUSUM) control chart. Next, Roberts [11] developed the exponentially weighted moving average (EWMA) control chart in 1959, which could detect minor changes in the process's mean. In 2004, Khoo [12] developed the moving average (MA) control chart, which computes the MA using the MA period (w) and detects small changes extremely effectively. All of the control charts mentioned above are better at detecting anomalies and recognizing small to moderate changes than the Shewhart control chart.

Recently, many researchers proposed mixing control charting approaches to improve the performance of these charts. The most obvious advantage of using mixed control charts is that they are more sensitive to detecting anomalies than classical control charts. As a result, they make it simpler to identify slight or slow changes in process parameters. For example, in 1990, the mixed Shewhart–EWMA control chart [13] was constructed to detect both small and large alterations in the process. In 2008, by integrating two MA statistics, Khoo and Wong [14] developed a double moving average (DMA) control chart, which enhances the MA control chart's capacity to identify small-to-medium shifts in a process of normal distribution. However, the DMA statistic reported in this study has an inaccurate variance. Later, in 2022, Alevizakos et al. [15] corrected this inaccurate variance in the DMA control chart. Taboran et al. [16] introduced the MA–EWMA control chart, which combines the smoothing properties of the MA with the sensitivity of the EWMA to improve the detection of short-term and long-term changes. Later that, a mixed EWMA–MA (MEM) control

chart [17] was designed by Sukprarungsee et al. in 2020 to detect the process's location and its application to real-life data sets. The covariance of the MA statistic was not considered in this work. This gap was later corrected by Raza et al. in [18]. Taboran and Sukparungsee [19] created a mixed EWMA–DMA (MEDM) control chart in 2023 to identify a slight shift in the mean process and used it on two real datasets: An industrial factory and the S&P 500 index. Later, Aslam et al. [20] proposed a mixed DMA–EWMA control chart for exponentially distributed quality by comparing it with the DMA control chart under exponential distribution and utilizing average run length (ARL) as the efficiency criterion. Following that, Saengsura et al. [21] designed a mixed DMA–CUSUM control chart to monitor mean shifts under both symmetric and asymmetrically distributed data. Asif et al. [22] proposed an accelerated failure time-based, risk-adjusted MA–EWMA control chart to enhance the monitoring of survival times in healthcare processes.

The majority of the charts mentioned above presuppose the normal distribution of the samples under observation. However, in real-world process monitoring settings, the normalcy assumption is frequently broken, and practitioners have little understanding of the underlying process's distribution. In this case, nonparametric control charts are an excellent alternative technique for addressing the aforementioned problem. One of the most popular testing tools for developing nonparametric control charts is the sign test because of its simplicity. For example, the sign test charts were initially proposed by Amin et al. [23]. They created Shewhart and CUSUM sign charts (Shewhart–sign and CUSUM–sign) to keep track of the process's locations. Yang et al. [24] created the EWMA–sign charts to identify the process's location. The generally weighted moving average (GWMA) control chart, which expands the EWMA chart by permitting weighting schemes and can improve sensitivity to identify small and moderate variations in the process's mean, was studied by Sheu and Lin [25]. On the basis of this work [25], Chakraborty *et al.* [26] proposed a GWMA–signed–rank chart that integrates the signed–rank statistic and the GWMA chart, yielding strong robustness versus abnormality. On the basis of this work [18], Raza et al. [27] developed a nonparametric EWMA–MA control chart using the sign test (EWMA–MA–sign or MEM–sign), in which the MA statistic is weighted toward the most recent w samples, since the effect of prior observations declines exponentially with time. Sudsutad et al. [28] designed the MEM–sign control chart based on the work of [17]. Furthermore, Raza et al. [29] created a nonparametric EWMA–MA control chart using signed–rank statistics to efficiently detect changes in the process's location. In 2021, Taboran et al. [30] studied the MA–double EWMA control chart with the Tukey statistic, which outperformed others in detecting mean shifts in both symmetric and non–symmetric processes. In 2024, Shanshool et al. [31] suggested a mixed Shewhart–EWMA control chart using the sign statistic (Shewhart–EWMA–sign) for the process's location and dispersion. As a result, it is clear that there has been relatively little study into developing mixed control charts using the sign statistic. Mahmood et al. [32] developed MA based location charts with modified successive sampling, demonstrating enhanced detection of small to moderate shifts in the process's quality. From research on related literature, it was found that the work of [19] did not take the covariance of the DMA statistic generated from the MEDM control chart into account; hence, the chart was confined to the independent attributes only, which may lead to inaccuracies in some real-world scenarios. To solve this problem and obtaining inspiration from the work of [19] and [15], we designed a distribution-free mixed EWMA–DMA sign (MEDM–sign) control chart for detecting changes in the process's location parameter that takes the interdependence between consecutive double MAs into account.

The remainder of the paper is arranged in the following manner: Section 2 includes the

corresponding design structures. Section 3 outlines how the proposed control chart's performance was measured. Section 4 shows the results and a discussion of the simulations. The comparative results are presented in Section 5 and Section 6 also provides applications of three real-world data examples from the sanitary industry, medical science, and the manufacturing industry with the proposed chart. Finally, the research concludes with a summary and some closing notes.

2. Construction of existing and nonparametric control charts

In this section, we provide the control charts and their attributes, which will be utilized throughout this work, including: the EWMA, MA, DMA, MEDM, and MEDM–sign control charts.

2.1. The EWMA control chart

In 1959, the EWMA control chart was introduced by Roberts [11], and showed performance in detecting small shifts. The Z_t statistic of the EWMA chart with a weighting parameter λ, where $\lambda \in (0, 1]$ for monitoring the process's mean is shown as

$$Z_t = \lambda X_t + (1 - \lambda)Z_{t-1}, \quad t = 1, 2, \ldots, \tag{2.1}$$

where X_t denotes independently and identically distributed (i.i.d.) random samples from the normal distribution with μ_0 and σ^2. The starting value is the process target, i.e., $Z_0 = \mu_0$. The expected and variance of the EWMA chart are given by

$$E(Z_t) = \mu_0 \quad \text{and} \quad V(Z_t) = \sigma^2 \left(\frac{\lambda}{2 - \lambda} \left(1 - (1 - \lambda)^{2t} \right) \right), \ t = 1, 2, \ldots. \tag{2.2}$$

If we take $t \to \infty$, then $(1 - \lambda)^{2t} \to 0$. This yields the following asymptotic variance:

$$V(Z_t) = \sigma^2 \left(\frac{\lambda}{2 - \lambda} \right). \tag{2.3}$$

The asymptotic control limits of the EWMA chart are calculated as follows:

$$UCL_1/LCL_1 = \mu_0 \pm L_1 \sqrt{\sigma^2 \left(\frac{\lambda}{2 - \lambda} \right)}, \tag{2.4}$$

where L_1 denotes a coefficient of the control limits of the EWMA chart. The process's mean and variance are denoted as μ_0 and σ^2, respectively.

2.2. The MA control chart

The MA chart is a handy tool in SPC and is capable of detecting small changes. It was proposed by Khoo in 2004 [12]. Let us assume that we have collected individual observations. Let X_t, $t = 1, 2, \ldots$, be i.i.d. random samples from the normal distribution. The MA_t statistic of the MA chart derived from the MA at each span w at time t is computed as follows:

$$MA_t = \begin{cases} \dfrac{1}{t} \displaystyle\sum_{j=1}^{t} X_j, & t < w, \\ \dfrac{1}{w} \displaystyle\sum_{j=t-w+1}^{t} X_j, & t \geq w. \end{cases} \tag{2.5}$$

The mean or expected and variance values of the MA_t statistic (2.5) are defined by

$$E(MA_t) = \mu_0 \qquad \text{and} \qquad V(MA_t) = \begin{cases} \dfrac{\sigma^2}{t}, & t < w, \\ \dfrac{\sigma^2}{w}, & t \geq w. \end{cases} \tag{2.6}$$

The covariance of the MA chart was studied by Alevizakos et al. [15] in 2020, i.e.,

$$Cov(MA_{j_1}, MA_{j_2}) = \begin{cases} \sigma^2 \Lambda_1(j_1, j_2), & 1 \leq j_1, j_2 \leq w-1, \\ \sigma^2 \Lambda_2(j_1, j_2), & 1 \leq j_1 \leq w-1, \ j_2 \geq w, \\ \sigma^2 \Lambda_2(j_1, j_2), & j_1, j_2 \geq w, \\ 0, & j_2 - j_1 \geq w, \end{cases} \tag{2.7}$$

where

$$\Lambda_1(j_1, j_2) = \frac{\min\{j_1, j_2\}}{j_1 j_2}, \qquad 1 \leq j_1, j_2 \leq w-1, \tag{2.8}$$

$$\Lambda_2(j_1, j_2) = \frac{\max\{0, j_1 - j_2 + w\}}{j_1 w}, \qquad 1 \leq j_1 \leq w-1, \ j_2 \geq w, \tag{2.9}$$

$$\Lambda_3(j_1, j_2) = \frac{\max\{0, j_1 - j_2 + w\}}{w^2}, \qquad j_1, j_2 \geq w. \tag{2.10}$$

The control limits of the MA chart are then established as

$$UCL_2/LCL_2 = \mu_0 \pm L_2 \sqrt{V(MA_t)}, \tag{2.11}$$

where L_2 denotes a coefficient of the control limits of the MA chart. The process's mean and variance are denoted as μ_0 and σ^2, respectively.

2.3. The DMA control c hart

We now provide the details of the DMA chart which was developed by Khoo et al. in 2008 [14] and corrected the variance by Alevizakos et al. [15]. Let us assume that we have collected individual observations. The DMA_t statistic of the DMA chart derived from the MA at each span (w) at time t is computed as

$$DMA_t = \begin{cases} \dfrac{1}{t} \displaystyle\sum_{j=1}^{t} MA_j, & t < w, \\ \dfrac{1}{w} \displaystyle\sum_{j=t-w+1}^{t} MA_j, & t \geq w, \end{cases} \tag{2.12}$$

where MA_t denotes the statistic of the MA chart, which is defined by (2.5). The expected and variance values of the DMA chart are defined by $E(DMA_t) = \mu_0$ and

$$V(DMA_t) = \begin{cases} \dfrac{\sigma^2}{t^2}\left[\displaystyle\sum_{j=1}^{t}\frac{1}{j} + \sum_{j_1=1}^{t-1}\sum_{j_2=j_1+1}^{t}\frac{2}{j_2}\right], & 1 \le t < w, \\ \dfrac{\sigma^2}{w^2}\Bigg[\displaystyle\sum_{j_1=t-w+1}^{w-1}\frac{1}{j_1} + \sum_{t-w+1\le j_1<j_2\le w-1}\frac{2}{j_2} + \frac{t-w+1}{w} \\ \quad + \displaystyle\sum_{j_1=t-w+1}^{w-1}\sum_{j_2=w}^{t}2\Lambda_2(j_1,j_2) + \sum_{w\le j_1<j_2\le t}2\Lambda_3(j_1,j_2)\Bigg], & w \le t < 2w-1, \\ \dfrac{\sigma^2}{w^2}\left[1 + \displaystyle\sum_{t-w+1\le j_1<j_2\le t}2\Lambda_3(j_1,j_2)\right], & t \ge 2w-1, \end{cases} \tag{2.13}$$

where $\Lambda_i(u_1, u_2)$ are given by (2.8)–(2.10) for $i = 1, 2, 3$, respectively. The covariance of the DMA chart is given by

$$Cov(DMA_{j_1}, DMA_{j_2}) = \begin{cases} \dfrac{\sigma^2}{j_1 j_2}\left[\displaystyle\sum_{u_1=1}^{j_1}\frac{1}{u_1} + \sum_{1\le u_1<u_2\le j_1}\frac{2}{u_2} + \sum_{u_1=1}^{j_1}\sum_{u_2=u_1+1}^{j_2}\frac{1}{u_2}\right], \\ \qquad 1 \le j_1, j_2 \le w-1, \\ \dfrac{\sigma^2}{j_1 w}\left[\displaystyle\sum_{u_1=1}^{j_1}\sum_{u_2=j_2-w+1}^{w-1}\Lambda_1(u_1,u_2) + \sum_{u_1=1}^{j_1}\sum_{u_2=w}^{j_2}\Lambda_2(u_1,u_2)\right], \\ \qquad w \le t < 2w-1,\ t-w+1 \le j_1 \le w-1,\ w \le j_2 \le t, \\ \dfrac{\sigma^2}{j_1 w}\Bigg[\displaystyle\sum_{u_1=j_1-w+1}^{j_2-w}\sum_{u_2=j_2-w+1}^{w-1}\Lambda_1(u_1,u_2) + \sum_{u_1=j_1-w+1}^{j_2-w}\sum_{u_2=w}^{j_2}\Lambda_2(u_1,u_2) \\ \quad + \displaystyle\sum_{u_1=j_2-w+1}^{w-1}\frac{1}{u_1} + \frac{j_1-w+1}{w} + \sum_{j_2-w+1\le u_1<u_2\le w-1}\frac{2}{u_2} \\ \quad + \displaystyle\sum_{u_1=j_2-w+1}^{w-1}\sum_{u_2=w}^{j_1}2\Lambda_2(u_1,u_2) + \sum_{w\le u_1<u_2\le j_1}2\Lambda_3(u_1,u_2) \\ \quad + \displaystyle\sum_{u_1=j_2-w+1}^{w-1}\sum_{u_2=j_1+1}^{j_2}\Lambda_3(u_1,u_2) + \sum_{u_1=w}^{j_1}\sum_{u_2=j_1+1}^{j_2}\Lambda_3(u_1,u_2)\Bigg], \\ \qquad w \le j_1 < j_2 < 2w-1, \\ \dfrac{\sigma^2}{w^2}\left[\displaystyle\sum_{u_1=j_1-w+1}^{w-1}\sum_{u_2=j_2-w+1}^{j_2}\Lambda_2(u_1,u_2) + \sum_{u_1=w}^{j_1}\sum_{u_2=j_2-w+1}^{j_2}\Lambda_3(u_1,u_2)\right] \\ \qquad w \le j_1 \le 2w-2,\ 2w-1 \le j_2 \le 3w-3, \\ \dfrac{\sigma^2}{w^2}\displaystyle\sum_{u_1=j_1-w+1}^{j_1}\sum_{u_2=j_2-w+1}^{j_2}\Lambda_3(u_1,u_2), \\ \qquad w \le u_1 < 2w-1,\ u_2 \ge 2w-1, \end{cases} \tag{2.14}$$

where $\Lambda_i(u_1, u_2)$ are given by (2.8)–(2.10) for $i = 1, 2, 3$, respectively. The control limits of the DMA chart are established as

$$UCL_3/LCL_3 = \mu_0 \pm L_3 \sqrt{V(DMA_t)}, \tag{2.15}$$

where L_3 denotes a coefficient of the control limits of the DMA chart. The process's mean and variance are denoted as μ_0 and σ^2, respectively.

2.4. The MEDM control chart

In 2023, Taboran and Sukparungsee [19] developed the MEDM control chart, in which the DMA_t statistic is used as input to the EWMA control chart to monitor the process's location. The $MEDM_t$ statistic of the MEDM control chart at time t is given as

$$MEDM_t = \lambda DMA_t + (1 - \lambda)MEDM_{t-1}, \quad t = 1, 2, \ldots, \tag{2.16}$$

where DMA_t denotes the DMA statistic at time t, λ is a weighting parameter with $\lambda \in (0, 1]$, and $MEDM_0$ denotes the initial value which is the process target such that $MEDM_0 = \mu_0 = \mu_{DMA}$. The variance formulation of the MEDM charting statistic shows that the DMA components are independent of one another. This technique might lead to false findings in practice because each DMA term of span w may incorporate information from $w - 1$ previous samples. Therefore, the MEDM chart should be adjusted to achieve correct control limits and results. In this section, we will modify the variance of the MEDM control chart by taking the DMA terms' dependency frame into account.

The $MEDM_t$ statistic (2.16) can be expressed as

$$MEDM_t = \lambda \sum_{j=0}^{t-1} (1 - \lambda)^j DMA_{t-j} + (1 - \lambda)^t MEDM_0. \tag{2.17}$$

The expected value of the $MEDM_t$ statistic is defined by

$$\begin{aligned} E(MEDM_t) &= \lambda \sum_{j=0}^{t-1} (1 - \lambda)^j E(DMA_{t-j}) + (1 - \lambda)^t E(MEDM_0) \\ &= \mu_0 \left(\lambda \sum_{j=0}^{t-1} (1 - \lambda)^j + (1 - \lambda)^{t-1} \right) = \mu_0 \left(\lambda \left(\frac{1 - (1 - \lambda)^t}{1 - (1 - \lambda)} \right) + (1 - \lambda)^t \right) = \mu_0. \end{aligned} \tag{2.18}$$

The revised variance formula of the $MEDM_t$ statistic is defined as follows:

$$\begin{aligned} V(MEDM_t) &= \lambda^2 \sum_{j=0}^{t-1} (1 - \lambda)^{2t} V(DMA_{t-j}) + 2\lambda^2 \sum_{1 \le j_1 < j_2 \le t} (1 - \lambda)^{t-j_1} (1 - \lambda)^{t-j_2} Cov(DMA_{j_1}, DMA_{j_2}) \\ &= \lambda^2 \sum_{j=0}^{t-1} (1 - \lambda)^{2t} V(DMA_j) + 2\lambda^2 \sum_{j_1=1}^{t-1} \sum_{j_2=j_1+1}^{t} (1 - \lambda)^{2t-j_1-j_2} Cov(DMA_{j_1}, DMA_{j_2}), \end{aligned} \tag{2.19}$$

where $V(DMA_t)$ and $Cov(DMA_{j_1}, DMA_{j_2})$ are defined by (2.13) and (2.14), respectively. The revised control limits of the MEDM control chart are then given as

$$UCL_4/LCL_4 = \mu_0 \pm L_4 \sqrt{V(MEDM_t)}, \tag{2.20}$$

where L_4 denotes a coefficient of the control limits of the MEDM control chart.

2.5. Nonparametric EWMA–DMA–sign (MEDM–sign) chart

Let X denote a specific feature with a target or median value of θ. Let Y denote a deviation of X from θ under probability $p = P(Y > 0)$. The process is called IC if $p = p_0 = P(Y \leq \theta) = P(Y > \theta) = 0.5$, while the process is called OOC if $p = p_1 \neq 0.5$. Let X_{jt}, $j = 1, 2, \ldots, n$, and $t = 1, 2, \ldots, m$, be the observation at time at time t in the j^{th} logical subgroup of size n, which is i.i.d. taken from X to survey the difference from the process's target value θ. The difference between X_{jt} and θ, i.e., $Y_{jt} = X_{jt} - \theta$, is inside groups defined by

$$Y_{jt} = X_{jt} - \theta \qquad \text{and} \qquad I_{jt} = \begin{cases} 1, & Y_{jt} > 0, \\ 0, & \text{otherwise.} \end{cases} \tag{2.21}$$

Suppose that S_t is the sign statistic, which is the total number of positive signs, i.e., $S_t = \sum_{j=1}^{n} I_{jt}$. It evaluates a binomial distribution with a parameter $(n, p_0) = (n, 0.5)$ for an IC process.

Next, a nonparametric MEDM–sign chart was constructed by integrating the MEDM chart and the sign test. First, the MA_{S_t} statistic of span w at time t is given as

$$MA_{S_t} = \begin{cases} \dfrac{1}{t}\displaystyle\sum_{j=1}^{t} S_i, & t < w, \\ \dfrac{1}{w}\displaystyle\sum_{j=t-w+1}^{t} S_i, & t \geq w, \end{cases} \tag{2.22}$$

where

$$E(MA_{S_t}) = \mu_0 = \frac{n}{2}, \qquad V(MA_{S_t}) = \begin{cases} \dfrac{n}{4t}, & t < w, \\ \dfrac{n}{4w}, & t \geq w, \end{cases} \tag{2.23}$$

and the covariance of the MA_{S_t} statistic is provided by

$$Cov(MA_{S_{j_1}}, MA_{S_{j_2}}) = \begin{cases} \dfrac{n\Lambda_1(j_1, j_2)}{4}, & 1 \leq j_1, j_2 \leq w - 1, \\ \dfrac{n\Lambda_2(j_1, j_2)}{4}, & 1 \leq j_1 \leq w - 1, \ j_2 \geq w, \\ \dfrac{n\Lambda_3(j_1, j_2)}{4}, & j_1, j_2 \geq w, \\ 0, & j_2 - j_1 \geq w, \end{cases} \tag{2.24}$$

where $\Lambda_i(j_1, j_2)$ are given by (2.8)–(2.10) for $i = 1, 2, 3$, respectively. Now, the DMA_{S_t} statistic of span w at time t is given as

$$DMA_{S_t} = \begin{cases} \dfrac{1}{t}\displaystyle\sum_{j=1}^{t} MA_{S_j}, & t < w, \\ \dfrac{1}{w}\displaystyle\sum_{j=t-w+1}^{t} MA_{S_j}, & t \geq w, \end{cases} \tag{2.25}$$

where $E(DMA_{S_t}) = n/2$, $V(DMA_{S_t})$ is given by (A.7), and the covariance of the DMA–sign control chart is given by (A.14). The $MEDM_{S_t}$ statistic is designed by

$$MEDM_{S_t} = \lambda DMA_{S_t} + (1 - \lambda) MEDM_{S_{t-1}}, \quad t = 1, 2, \ldots, \tag{2.26}$$

where λ denotes a smoothing parameter with $\lambda \in (0, 1]$, $MEDM_{S_0} = \mu_0 = n/2$. Next, we show that the expected and variance values of the $MEDM_{S_t}$ statistic of the MEDM–sign chart. The statistic (2.26) can be rewritten as

$$MEDM_{S_t} = \lambda \sum_{j=0}^{t-1} (1-\lambda)^j DMA_{S_{t-j}} + (1-\lambda)^t MEDM_{S_0}. \tag{2.27}$$

It is easy to show that the expected value $E(MEDM_{S_t})$. The expected value of the $MEDM_{S_t}$ statistic can be then calculated as follows:

$$E(MEDM_{S_t}) = \lambda \sum_{j=0}^{t-1} (1-\lambda)^j E(DMA_{S_{t-j}}) + (1-\lambda)^t E(MEDM_{S_0}) = \frac{n}{2}. \tag{2.28}$$

The revised variance formula of the $MEDM_{S_t}$ statistic is defined as shown below:

$$V(MEDM_{S_t}) = \lambda^2 \sum_{j=0}^{t-1} (1-\lambda)^{2t} V(DMA_{S_j}) + 2\lambda^2 \sum_{j_1=1}^{t-1} \sum_{j_2=j_1+1}^{t} (1-\lambda)^{2t-j_1-j_2} Cov(DMA_{S_{j_1}}, DMA_{S_{j_2}}), \tag{2.29}$$

where $V(DMA_{S_j})$ and $Cov(DMA_{S_{j_1}}, DMA_{S_{j_2}})$ are denoted by (A.7) and (A.14), respectively. The revised control limits of the MEDM–sign control chart are then given as

$$UCL_5/LCL_5 = \frac{n}{2} \pm L_5 \sqrt{V(MEDM_{S_t})}, \tag{2.30}$$

where L_5 denotes a coefficient of the control limits of the MEDM–sign control chart. The MEDM–sign chart is generated by plotting $MEDM_{S_t}$ against the respective control limits. If $MEDM_{S_t}$ drops outside the control limits, the process is considered to be OOC. Otherwise, the process is IC; that is, if $LCL_{5_t} < MEDM_{S_t} < UCL_{5_t}$. This design seeks to enhance the process monitoring performance by achieving an effective balance between sensitivity and stability.

3. Performance evaluation of the MEDM–sign chart

The run length (RL) profile and its related properties are commonly used to measure the performance of a control chart. The effectiveness of a control chart is measured by its ability to promptly and accurately identify shifts in the process's mean. The sensitivity of control charts may be evaluated using various performance measures based on run length distributions such as ARL, standard deviation of run length (S-DRL), and median run length (MRL). In addition, other tools are used to evaluate the overall performance of control charts, including average extra quadratic loss (AEQL), relative mean index (RMI), and performance comparison index (PCI).

The ARL value is widely used to analyze the performance of control charts. ARL is the predicted number of plotted statistics before an OOC signal is received for the first time; see [1]. It is the most popular performance measurement instrument. The control charts will signal a false alarm if the process is IC; it has a large value of ARL. It is said to be ARL_0. In contrast, if the process is OOC, the ARL value is low, and the control charts will rapidly detect the change, demonstrating that the chart is successful at recognizing deviations from the target mean. It is said to be ARL_1. Because of the ARL's

skewness distribution, it is used to quantify the control chart's performance, and it is recommended to utilize percentiles of the RL attributes to assess performance, such as S-DRL which measures the variability, MRL which is the middle value of RLs; see [33–35]. The control chart via the minimal values of ARL_1, MRL_1, and $SDRL_1$ is more effective at immediately detecting changes in the process for a specific ARL_0. In this work, ARL, S-DRL, and MRL values were obtained using the Monte Carlo (MC) simulation approach with R software, where $ARL_0 \approxeq 370$, as follows:

$$ARL = \frac{1}{1 - P(LCL_5 \leq MEDM_{S_t} \leq UCL_5)}, \tag{3.1}$$

and

$$ARL = \frac{\sum_{k=1}^{N} RL_k}{N}, \quad S - DRL = \sqrt{\frac{\sum_{k=1}^{N}(RL_k)^2}{N} - (ARL)^2}, \quad MRL = Median(RL), \tag{3.2}$$

where k is presented as number of experimental repetitions, so RL_t represents the number of simulation repeats. The redundant RL_t should be changed to RL_k, which is necessary before the first sample exceeds the OOC limits, and N denotes the number of repetitions simulated. Nevertheless, if the amount of the change is vague but can be fairly anticipated to fall within a specific range, in this situation, different tools can help analyze the overall performance within that range, including AEQL, PCI, and RMI. AEQL is used to evaluate a chart's performance over a range of variations considered during the workflow; it is based on the loss function. The mathematical expression of AEQL is given by

$$AEQL = \frac{1}{\Delta} \sum_{\delta=\delta_{\min}}^{\delta=\delta_{\max}} \delta^2 \times ARL(\delta) \quad \text{where} \quad \Delta = \delta_{\max} - \delta_{\min}, \tag{3.3}$$

where $ARL(\delta)$ denotes the value of ARL for a certain change δ, δ refers to the number of shifts observed in the process, and $\delta_{\max}$ and $\delta_{\min}$ represent the maximum and minimum shifts regarded in the location process, respectively. A smaller value of AEQL indicates that the control chart is performing better. Next, the RMI value is the performance tool, which was suggested by Han and Tsung [36]. The value of RMI depends on the relative differences in the ARL_1, which is given by

$$RMI = \frac{1}{N} \sum_{i=1}^{N} \frac{ARL(\delta_i) - ARL^*(\delta_i)}{ARL^*(\delta_i)}, \tag{3.4}$$

where N denotes the total number of shifts considered in the process, $ARL(\delta_i)$ denotes the value of ARL for a control chart satisfying a certain shift δ_i, and $ARL^*(\delta_i)$ denotes the value of a control chart with the smallest value of ARL_1 among all of the emulating control charts for the assigned shift. Similarly, the control chart with respect to the smallest RMI value is thought to be more efficient than the others. Finally, the value of PCI is defined as the ratio of a chart's AEQL value to the benchmark chart's AEQL, which is recommended by the work in [37]. A chart with a low PCI value is chosen over other charts. It is given by

$$PCI = \frac{AEQL}{AEQL_{\text{benchmark}}}. \tag{3.5}$$

The value of the RL profile for the control chart may be calculated using many methods, including the integral equation, the Markov chain method, and MC simulation. In this paper, we will use MC

simulation to calculate the RL profile of all control charts. This method is preferred over other estimating strategies because it is precise and adaptable enough to handle a wide range of circumstances. The following details the steps of this procedure are shown below.

(1) Generate the sample size (n) for each round of the experiment using 2000 random numbers from a given distribution under the parameters n, w, and λ with the mean adjusted from μ to μ_1, i.e., $\mu_1 = \mu + \delta\sigma$.
(2) The number of experiment repetitions is set to $N = 200000$ to ensure stable run length estimates while maintaining a reasonable computational cost.
(3) To achieve the desired $ARL_0 \simeq 370$, set an arbitrary value of L while keeping the other design parameters, n, w, and λ, constant.
(4) Compute the DMA_{S_t} using Eq. (2.25) and then define the monitoring statistic $MEDM_{S_t}$, which is given by (2.26).
(5) Estimate the control limits and compare them with the charting statistics $MEDM_{S_t}$.
(6) Count how many samples fall under the control limits before the MEDM–sign control chart sends the first OOC signal; this count is the single value of RL.
(7) Repeat Steps (1) to (5) with 200000 replications (N) to compute the characteristic values of RL, including ARL, S-DRL, and MRL.

Table 1. The value of L_6 for the MEDM–sign control chart for varying (n, w, λ) at $ARL_0 \simeq 370$ under the $Normal(0, 1)$ distribution.

n	λ	MEDM–sign control chart									
		$w = 2$	$w = 3$	$w = 4$	$w = 5$	$w = 6$	$w = 7$	$w = 8$	$w = 9$	$w = 10$	$w = 15$
5	0.05	4.694	6.785	8.803	10.756	12.674	14.485	16.271	18.006	19.683	27.417
	0.20	4.999	6.975	8.736	10.338	11.803	13.138	14.367	15.514	16.583	21.106
	0.25	4.950	6.828	8.4736	9.935	11.252	12.436	13.531	14.536	15.478	19.511
10	0.05	4.695	6.788	8.805	10.756	12.642	14.479	16.265	17.995	19.681	27.405
	0.20	5.038	7.003	8.775	10.378	11.829	13.159	14.389	15.517	16.584	21.085
	0.25	4.998	6.871	8.517	9.975	11.285	12.468	13.551	14.548	15.485	19.396
15	0.05	4.696	6.793	8.909	10.761	12.654	14.489	16.269	17.998	19.681	27.405
	0.20	5.052	7.016	8.787	10.382	11.839	13.165	14.395	15.532	16.598	21.098
	0.25	5.017	6.885	8.527	9.985	11.295	12.478	13.557	14.557	15.488	19.415

For Step (1), given $p = p_0 = 0.5$ for computing the value of ARL_0, while ARL_1 values are computed by repeating Steps (1) to (7) under $p = p_1 \neq 0.5$. Our simulation study uses $\lambda = 0.05, 0.20$, and 0.25; span $w = 2, 3, 4, 5, 6, 7, 8, 9, 10, 15$; and a sample size $n = 5, 10, 15$. Each chart's control limits (L) are calibrated to achieve an IC ARL of approximately $ARL_0 \simeq 370$, ensuring a fair comparison across different parameter settings. The value L is selected using an iterative procedure, which is satisfied by the bisection technique, i.e., $L = (L_{\text{lower}} + L_{\text{upper}})/2$. Calculate the equivalent $ARL_0 \simeq 370$ by substituting the value L into the simulation. If $ARL_0 < 370$, L is increased by setting $L_{\text{lower}} = L$; otherwise, if $ARL_0 > 370$, $L_{\text{upper}} = L$. This procedure is repeated until a value of L is obtained such that the resulting IC ARL satisfies $ARL_0 \simeq 370$. Table 1 shows the control limit coefficient (L) of the MEDM–sign control chart for varying sample sizes (n) and parameters (w, λ) at $ARL_0 \simeq 370$. When λ

and n are fixed, the limit coefficient (L) increases while the span (w) increases. It has also been noticed that the value of L increases with n for a constant value of w. For effective monitoring of minor shifts in the process, it is generally advisable to select a relatively large w and a small smoothing parameter λ. A larger w emphasizes the contribution of recent observations, improving responsiveness, whereas a smaller λ limits the memory of past data, facilitating faster adaptation to new changes. This parameter configuration has been shown in simulation studies to optimize the detection speed while maintaining acceptable false alarm rates.

4. Results and discussion of simulations

This study evaluated the performance of the MEDM–sign control chart compared with the Shewhart, EWMA, MA, DMA, MEM, and MEDM control charts when the process was not under control. This work includes four distributions: Two symmetric distributions ($Normal(0, 1)$ and $Laplace(0, 1)$) and two asymmetric distributions ($Exponential(1)$ and $Gamma(4, 1)$). The four distributions are chosen to evaluate the robustness of the proposed control charts across diverse data-generating mechanisms. These distributions are widely used due to their mathematical properties and their vast applicability in simulating various occurrences. The normal distribution represents a large number of random variables, describes many natural phenomena, serves as a foundation for statistics and probability theory, underpins the central limit theorem, and supports numerous statistical methods. The Laplace distribution is widely recognized as an effective probability distribution for modeling random phenomena in various fields, such as engineering, finance, biomedical science, environmental science, and other related areas. The exponential distribution is frequently utilized in commercial and scientific studies because it provides significant insights into the behavior of time-dependent events and survival analysis. The gamma distribution is widely used in many fields such as engineering, finance, healthcare, and statistics, particularly for modeling waiting times and reliability analyses. We present the performance of the proposed control chart by using a sample size of 2000 and 200000 iterations in the MC simulations technique with $ARL_0 \simeq 370$. The RL profiles of all the control charts are obtained through simulations with $\lambda = 0.25$; $n = 5, 10, 15$; $\delta = 0, \pm 0.05 \pm 0.10, \pm 0.25, \pm 0.50, \pm 0.75, \pm 1.00, \pm 1.50, \pm 2.00, \pm 3.00, \pm 4.00$; and $w = 2, 5, 8, 10, 15$, for various distributions such as $Normal(0, 1)$, $Laplace(0, 1)$, $Exponential(1)$, and $Gamma(4, 1)$, as shown in Tables 2–13. The advantage of all control charts was evaluated using ARL based on the zero-state, which was defined as the minimum average run length (ARL_1). Tables 2–4 present the simulation results of ARL performance for $w = 2, 5, 8, 10, 15$ and $n = 5, 10, 15$ when the data's distribution is $Normal(0, 1)$. While the simulation results of ARL performance for varying w and n when the data's distribution is $Laplace(0, 1)$ are shown in Tables 5–7. In addition, the distributions of $Exponential(1)$, and $Gamma(4, 1)$ are similar, as shown in Tables 8–10 and Tables 11–13, respectively. Note that, if speedy detection of small changes is desired, a large value of w is often preferred. Furthermore, Table 14 displays the overall performance efficacy of the MEDM–sign control chart under various distributions by varying $w = 2, 5, 8, 10, 15$; $n = 5, 10, 15$; and $\lambda = 0.25$.

Table 2. The ARL_1 performance of the MEDM–sign control chart under the $Normal(0, 1)$ distribution by varying $w = \{2, 5, 8, 10, 15\}$ and given $ARL_0 = 370$, $\lambda = 0.25$, and $n = 5$.

Shift	$(w, L) = (2, 4.950)$			$(w, L) = (5, 9.935)$			$(w, L) = (8, 13.531)$			$(w, L) = (10, 15.478)$			$(w, L) = (15, 19.511)$		
	ARL	S-DRL	MRL	ARL	S-DRL	MRL	ARL	S-DRL	MRL	ARL	S-DRL	MRL	ARL	S-DRL	MRL
-4.00	0.00	0.00	0	0.00	0.00	0	0.00	0.00	0	0.00	0.00	0	0.00	0.00	0
-3.00	0.01	0.00	0	0.01	0.00	0	0.00	0.00	0	0.00	0.00	0	0.00	0.00	0
-2.00	0.24	0.00	0	0.12	0.00	0	0.02	0.00	0	0.01	0.00	0	0.01	0.00	0
-1.50	0.73	0.00	1	0.41	0.00	0	0.18	0.00	0	0.11	0.00	0	0.07	0.00	0
-1.00	2.07	0.00	2	1.40	0.00	1	1.01	0.00	0	0.79	0.00	0	0.56	0.00	0
-0.75	3.94	0.01	3	2.82	0.01	1	2.33	0.01	1	2.01	0.01	0	1.53	0.01	0
-0.50	9.82	0.02	7	7.16	0.02	5	6.08	0.02	3	5.53	0.02	2	4.50	0.02	1
-0.25	45.69	0.10	32	35.04	0.09	23	28.86	0.08	17	25.84	0.08	14	20.39	0.07	5
-0.10	189.99	0.43	131	167.90	0.43	106	149.51	0.42	84	138.62	0.41	70	117.35	0.40	36
-0.05	301.95	0.68	209	287.86	0.73	183	276.10	0.77	156	268.39	0.79	136	250.81	0.84	75
0.00	370.57	0.82	258	370.02	0.92	236	370.30	0.99	210	370.81	1.05	190	370.08	1.17	115
0.05	301.38	0.68	208	288.66	0.73	183	276.33	0.77	155	268.35	0.79	135	250.91	0.84	75
0.10	190.37	0.43	132	167.70	0.43	106	149.22	0.42	84	138.58	0.41	70	117.74	0.40	36
0.25	45.41	0.10	32	34.98	0.09	22	28.72	0.08	17	25.72	0.07	14	20.35	0.07	5
0.50	9.79	0.02	7	7.15	0.02	5	6.05	0.02	3	5.49	0.02	2	4.48	0.02	1
0.75	3.93	0.01	3	2.80	0.01	1	2.31	0.01	1	1.99	0.01	0	1.52	0.01	0
1.00	2.06	0.00	2	1.38	0.00	1	1.00	0.00	0	0.78	0.00	0	0.56	0.00	0
1.50	0.72	0.00	0	0.40	0.00	0	0.18	0.00	0	0.11	0.00	0	0.07	0.00	0
2.00	0.23	0.00	0	0.12	0.00	0	0.02	0.00	0	0.01	0.00	0	0.01	0.00	0
3.00	0.01	0.00	0	0.01	0.00	0	0.00	0.00	0	0.00	0.00	0	0.00	0.00	0
4.00	0.00	0.00	0	0.00	0.00	0	0.00	0.00	0	0.00	0.00	0	0.00	0.00	0

Table 3. The ARL_1 performance of the MEDM–sign control chart under the $Normal(0, 1)$ distribution by varying $w = \{2, 5, 8, 10, 15\}$ and given $ARL_0 = 370$, $\lambda = 0.25$, and $n = 10$.

Shift	$(w, L) = (2, 4.998)$			$(w, L) = (5, 9.975)$			$(w, L) = (8, 13.551)$			$(w, L) = (10, 15.485)$			$(w, L) = (15, 19.396)$		
	ARL	S-DRL	MRL	ARL	S-DRL	MRL	ARL	S-DRL	MRL	ARL	S-DRL	MRL	ARL	S-DRL	MRL
-4.00	0.00	0.00	0	0.00	0.00	0	0.00	0.00	0	0.00	0.00	0	0.00	0.00	0
-3.00	0.00	0.00	0	0.00	0.00	0	0.00	0.00	0	0.00	0.00	0	0.00	0.00	0
-2.00	0.02	0.00	0	0.00	0.00	0	0.00	0.00	0	0.00	0.00	0	0.00	0.00	0
-1.50	0.15	0.00	0	0.02	0.00	0	0.02	0.00	0	0.00	0.00	0	0.00	0.00	0
-1.00	0.67	0.00	0	0.35	0.00	0	0.26	0.00	0	0.15	0.00	0	0.09	0.00	0
-0.75	1.49	0.00	1	1.05	0.00	0	0.82	0.00	0	0.61	0.00	0	0.41	0.00	0
-0.50	4.15	0.01	3	3.12	0.01	2	2.66	0.01	1	2.34	0.01	1	1.78	0.01	0
-0.25	21.13	0.05	15	15.84	0.04	11	13.14	0.04	8	11.90	0.03	6	9.76	0.03	3
-0.10	123.78	0.28	85	103.58	0.26	66	88.54	0.25	50	80.73	0.24	42	65.66	0.22	24
-0.05	253.32	0.57	174	233.57	0.59	148	216.65	0.61	123	205.69	0.61	106	183.44	0.61	64
0.00	370.20	0.82	256	370.46	0.92	237	370.50	0.99	212	370.89	1.04	193	370.12	1.14	132
0.05	253.77	0.57	175	235.16	0.60	149	217.25	0.61	123	206.94	0.61	106	184.73	0.61	63
0.10	123.87	0.28	86	103.76	0.27	66	88.87	0.25	51	80.80	0.24	42	65.55	0.22	24
0.25	21.07	0.05	15	15.88	0.04	11	13.16	0.04	8	11.92	0.03	6	9.73	0.03	3
0.50	4.10	0.01	3	3.12	0.01	2	2.65	0.01	1	2.33	0.01	1	1.78	0.01	0
0.75	1.48	0.00	1	1.04	0.00	0	0.82	0.00	0	0.61	0.00	0	0.41	0.00	0
1.00	0.67	0.00	0	0.35	0.00	0	0.26	0.00	0	0.15	0.00	0	0.09	0.00	0
1.50	0.14	0.00	0	0.03	0.00	0	0.02	0.00	0	0.00	0.00	0	0.00	0.00	0
2.00	0.02	0.00	0	0.00	0.00	0	0.00	0.00	0	0.00	0.00	0	0.00	0.00	0
3.00	0.00	0.00	0	0.00	0.00	0	0.00	0.00	0	0.00	0.00	0	0.00	0.00	0
4.00	0.00	0.00	0	0.00	0.00	0	0.00	0.00	0	0.00	0.00	0	0.00	0.00	0

Table 4. The ARL_1 performance of the MEDM–sign control chart under the $Normal(0, 1)$ distribution by varying $w = \{2, 5, 8, 10, 15\}$ and given $ARL_0 = 370$, $\lambda = 0.25$, and $n = 15$.

Shift	$(w, L) = (2, 5.017)$			$(w, L) = (5, 9.985)$			$(w, L) = (8, 13.557)$			$(w, L) = (10, 15.488)$			$(w, L) = (15, 19.415)$		
	ARL	S-DRL	MRL	ARL	S-DRL	MRL	ARL	S-DRL	MRL	ARL	S-DRL	MRL	ARL	S-DRL	MRL
-4.00	0.00	0.00	0	0.00	0.00	0	0.00	0.00	0	0.00	0.00	0	0.00	0.00	0
-3.00	0.00	0.00	0	0.00	0.00	0	0.00	0.00	0	0.00	0.00	0	0.00	0.00	0
-2.00	0.00	0.00	0	0.00	0.00	0	0.00	0.00	0	0.00	0.00	0	0.00	0.00	0
-1.50	0.02	0.00	0	0.00	0.00	0	0.00	0.00	0	0.00	0.00	0	0.00	0.00	0
-1.00	0.24	0.00	0	0.10	0.00	0	0.06	0.00	0	0.03	0.00	0	0.02	0.00	0
-0.75	0.75	0.00	0	0.47	0.00	0	0.33	0.00	0	0.24	0.00	0	0.16	0.00	0
-0.50	2.44	0.01	2	1.83	0.01	1	1.50	0.01	0	1.28	0.01	0	0.92	0.00	0
-0.25	13.13	0.03	10	9.78	0.02	7	8.26	0.02	4	7.58	0.02	3	6.27	0.02	2
-0.10	89.74	0.20	62	72.68	0.19	46	61.07	0.17	35	55.25	0.16	29	44.43	0.14	17
-0.05	218.23	0.49	151	195.22	0.50	124	177.16	0.50	100	166.31	0.49	86	144.78	0.48	51
0.00	370.93	0.82	257	370.21	0.92	237	370.09	0.99	213	370.53	1.04	195	370.29	1.14	132
0.05	218.35	0.49	151	195.66	0.50	124	176.44	0.49	100	166.03	0.49	85	143.89	0.48	50
0.10	90.18	0.20	63	72.82	0.19	46	61.14	0.17	35	55.26	0.16	29	44.51	0.15	17
0.25	13.16	0.03	10	9.78	0.02	7	8.25	0.02	4	7.56	0.02	3	6.25	0.02	2
0.50	2.43	0.01	2	1.82	0.01	1	1.48	0.01	0	1.26	0.01	0	0.91	0.01	0
0.75	0.75	0.00	0	0.46	0.00	0	0.33	0.00	0	0.23	0.00	0	0.15	0.00	0
1.00	0.24	0.00	0	0.10	0.00	0	0.06	0.00	0	0.04	0.00	0	0.02	0.00	0
1.50	0.02	0.00	0	0.00	0.00	0	0.00	0.00	0	0.00	0.00	0	0.00	0.00	0
2.00	0.00	0.00	0	0.00	0.00	0	0.00	0.00	0	0.00	0.00	0	0.00	0.00	0
3.00	0.00	0.00	0	0.00	0.00	0	0.00	0.00	0	0.00	0.00	0	0.00	0.00	0
4.00	0.00	0.00	0	0.00	0.00	0	0.00	0.00	0	0.00	0.00	0	0.00	0.00	0

Table 5. The ARL_1 performance of the MEDM–sign control chart under the $Laplace(0, 1)$ distribution by varying $w = \{2, 5, 8, 10, 15\}$ and given $ARL_0 = 370$, $\lambda = 0.25$, and $n = 5$.

Shift	$(w, L) = (2, 4.951)$			$(w, L) = (5, 9.930)$			$(w, L) = (8, 13.525)$			$(w, L) = (10, 15.465)$			$(w, L) = (15, 19.497)$		
	ARL	S-DRL	MRL	ARL	S-DRL	MRL	ARL	S-DRL	MRL	ARL	S-DRL	MRL	ARL	S-DRL	MRL
-4.00	0.09	0.00	0	0.05	0.00	0	0.00	0.00	0	0.00	0.00	0	0.00	0.00	0
-3.00	0.26	0.00	0	0.13	0.00	0	0.03	0.00	0	0.01	0.00	0	0.01	0.00	0
-2.00	0.73	0.00	1	0.41	0.00	0	0.18	0.00	0	0.11	0.00	0	0.06	0.00	0
-1.50	1.28	0.00	1	0.79	0.00	0	0.48	0.00	0	0.34	0.00	0	0.21	0.00	0
-1.00	2.62	0.01	2	1.78	0.01	1	1.39	0.01	0	1.13	0.01	0	0.80	0.00	0
-0.75	4.33	0.01	3	3.06	0.01	1	2.57	0.01	1	2.23	0.01	0	1.69	0.01	0
-0.50	9.20	0.02	7	6.64	0.02	4	5.64	0.02	3	5.11	0.02	2	4.15	0.02	1
-0.25	35.68	0.08	25	27.05	0.07	18	22.23	0.06	14	19.91	0.06	11	15.81	0.05	28
-0.10	155.91	0.35	109	133.36	0.34	84	116.37	0.33	65	106.91	0.32	54	88.31	0.30	28
-0.05	276.88	0.62	192	259.02	0.66	164	244.18	0.68	139	234.92	0.69	120	213.49	0.72	64
0.00	370.28	0.82	257	370.28	0.92	236	370.69	0.99	211	370.01	1.05	190	370.11	1.17	115
0.05	275.65	0.62	191	258.28	0.66	164	242.87	0.68	137	232.84	0.69	118	212.53	0.72	64
0.10	155.40	0.35	108	133.26	0.34	84	116.53	0.33	65	106.81	0.32	54	87.94	0.30	27
0.25	36.65	0.08	25	27.11	0.07	18	22.29	0.06	14	19.95	0.06	11	15.76	0.05	4
0.50	9.19	0.02	7	6.34	0.02	4	5.66	0.02	3	5.13	0.02	2	4.16	0.01	1
0.75	4.32	0.01	3	3.06	0.01	1	2.58	0.01	1	2.25	0.01	0	1.71	0.01	0
1.00	2.62	0.01	2	1.79	0.01	1	1.40	0.01	0	1.13	0.01	0	0.80	0.00	0
1.50	1.29	0.00	1	0.79	0.00	0	0.49	0.00	0	0.34	0.00	0	0.22	0.00	0
2.00	0.73	0.00	1	0.41	0.00	0	0.18	0.00	0	0.11	0.00	0	0.07	0.00	0
3.00	0.26	0.00	0	0.13	0.00	0	0.03	0.00	0	0.01	0.00	0	0.01	0.00	0
4.00	0.09	0.00	0	0.05	0.00	0	0.00	0.00	0	0.00	0.00	0	0.00	0.00	0

Table 6. The ARL_1 performance of the MEDM–sign control chart under the $Laplace(0, 1)$ distribution by varying $w = \{2, 5, 8, 10, 15\}$ and given $ARL_0 = 370$, $\lambda = 0.25$, and $n = 10$.

Shift	$(w, L) = (2, 4.999)$			$(w, L) = (5, 9.969)$			$(w, L) = (8, 13.549)$			$(w, L) = (10, 15.479)$			$(w, L) = (15, 19.406)$		
	ARL	S-DRL	MRL	ARL	S-DRL	MRL	ARL	S-DRL	MRL	ARL	S-DRL	MRL	ARL	S-DRL	MRL
-4.00	0.00	0.00	0	0.00	0.00	0	0.00	0.00	0	0.00	0.00	0	0.00	0.00	0
-3.00	0.03	0.00	0	0.00	0.00	0	0.00	0.00	0	0.00	0.00	0	0.00	0.00	0
-2.00	0.15	0.00	0	0.03	0.00	0	0.02	0.00	0	0.01	0.00	0	0.00	0.00	0
-1.50	0.35	0.00	0	0.13	0.00	0	0.09	0.00	0	0.04	0.00	0	0.02	0.00	0
-1.00	0.91	0.00	1	0.55	0.00	0	0.41	0.00	0	0.27	0.00	0	0.17	0.00	0
-0.75	1.66	0.00	0	1.20	0.01	0	0.94	0.00	0	0.73	0.00	0	0.49	0.00	0
-0.50	3.83	0.01	3	2.91	0.01	2	2.45	0.01	0	2.13	0.01	1	1.63	0.01	0
-0.25	16.19	0.03	12	12.08	0.03	8	10.08	0.03	6	9.19	0.03	4	7.59	0.02	2
-0.10	93.78	0.21	65	75.99	0.19	48	64.14	0.18	37	58.00	0.17	30	46.67	0.15	18
-0.05	217.83	0.50	149	195.36	0.50	123	177.63	0.50	100	166.87	0.49	85	144.84	0.48	51
0.00	370.42	0.42	256	370.20	0.92	236	370.77	0.99	213	370.21	1.04	193	370.34	1.14	132
0.05	217.26	0.49	158	194.63	0.50	123	176.91	0.50	101	165.74	0.49	86	144.14	0.48	50
0.10	93.63	0.21	65	76.22	0.19	49	64.23	0.18	37	58.01	0.17	30	46.61	0.15	17
0.25	16.10	0.03	12	12.06	0.03	8	10.05	0.03	6	9.15	0.03	4	7.58	0.02	2
0.50	3.82	0.01	3	2.91	0.01	2	2.45	0.01	1	2.15	0.01	1	1.62	0.01	0
0.75	1.66	0.00	1	1.20	0.00	0	0.94	0.00	0	0.73	0.00	0	0.49	0.00	0
1.00	0.90	0.00	1	0.55	0.00	0	0.41	0.00	0	0.27	0.00	0	0.17	0.00	0
1.50	0.35	0.00	0	0.12	0.00	0	0.09	0.00	0	0.04	0.00	0	0.02	0.00	0
2.00	0.15	0.00	0	0.03	0.00	0	0.02	0.00	0	0.01	0.00	0	0.00	0.00	0
3.00	0.02	0.00	0	0.00	0.00	0	0.00	0.00	0	0.00	0.00	0	0.00	0.00	0
4.00	0.00	0.00	0	0.00	0.00	0	0.00	0.00	0	0.00	0.00	0	0.00	0.00	0

Table 7. The ARL_1 performance of the MEDM–sign control chart under the $Laplace(0, 1)$ distribution by varying $w = \{2, 5, 8, 10, 15\}$ and given $ARL_0 = 370$, $\lambda = 0.25$, and $n = 15$.

Shift	$(w, L) = (2, 5.016)$			$(w, L) = (5, 9.988)$			$(w, L) = (8, 13.555)$			$(w, L) = (10, 15.489)$			$(w, L) = (15, 19.415)$		
	ARL	S-DRL	MRL	ARL	S-DRL	MRL	ARL	S-DRL	MRL	ARL	S-DRL	MRL	ARL	S-DRL	MRL
-4.00	0.00	0.00	0	0.00	0.00	0	0.00	0.00	0	0.00	0.00	0	0.00	0.00	0
-3.00	0.00	0.00	0	0.00	0.00	0	0.00	0.00	0	0.00	0.00	0	0.00	0.00	0
-2.00	0.02	0.00	0	0.00	0.00	0	0.00	0.00	0	0.00	0.00	0	0.00	0.00	0
-1.50	0.08	0.00	0	0.02	0.00	0	0.01	0.00	0	0.01	0.00	0	0.00	0.00	0
-1.00	0.38	0.00	0	0.19	0.00	0	0.12	0.00	0	0.08	0.00	0	0.05	0.00	0
-0.75	0.86	0.00	1	0.56	0.00	0	0.40	0.00	0	0.29	0.00	0	0.20	0.00	0
-0.50	2.23	0.01	2	1.68	0.01	1	1.36	0.01	0	1.15	0.01	0	0.82	0.00	0
-0.25	9.89	0.02	7	7.42	0.02	5	6.32	0.02	3	5.80	0.02	2	4.76	0.02	1
-0.10	64.94	0.14	45	51.45	0.13	33	42.39	0.12	24	38.11	0.11	21	30.50	0.10	10
-0.05	178.99	0.41	123	156.02	0.40	99	137.66	0.39	78	127.40	0.38	65	107.44	0.36	37
0.00	370.90	0.83	256	370.73	0.92	237	370.07	0.99	213	370.73	1.04	195	370.57	1.14	134
0.05	178.49	0.40	123	156.60	0.40	99	137.90	0.39	78	127.88	0.38	66	108.24	0.36	39
0.10	65.11	0.15	46	51.69	0.13	33	42.86	0.12	25	38.64	0.11	21	30.88	0.10	11
0.25	9.95	0.02	8	7.45	0.02	5	6.34	0.02	3	5.83	0.02	2	4.80	0.02	1
0.50	2.24	0.01	2	1.70	0.01	1	1.37	0.01	0	1.16	0.01	0	0.83	0.00	0
0.75	0.86	0.00	1	0.56	0.00	0	0.40	0.00	0	0.30	0.00	0	0.20	0.00	0
1.00	0.38	0.00	0	0.19	0.00	0	0.12	0.00	0	0.08	0.00	0	0.05	0.00	0
1.50	0.08	0.00	0	0.02	0.00	0	0.01	0.00	0	0.01	0.00	0	0.00	0.00	0
2.00	0.02	0.00	0	0.00	0.00	0	0.00	0.00	0	0.00	0.00	0	0.00	0.00	0
3.00	0.00	0.00	0	0.00	0.00	0	0.00	0.00	0	0.00	0.00	0	0.00	0.00	0
4.00	0.00	0.00	0	0.00	0.00	0	0.00	0.00	0	0.00	0.00	0	0.00	0.00	0

Table 8. The ARL_1 performance of the MEDM–sign control chart under the *Exponential*(1) distribution by varying $w = \{2, 5, 8, 10, 15\}$ and given $ARL_0 = 370$, $\lambda = 0.25$, and $n = 5$.

Shift	$(w, L) = (2, 7.724)$			$(w, L) = (5, 16.015)$			$(w, L) = (8, 23.502)$			$(w, L) = (10, 28.061)$			$(w, L) = (15, 38.581)$		
	ARL	S-DRL	MRL	ARL	S-DRL	MRL	ARL	S-DRL	MRL	ARL	S-DRL	MRL	ARL	S-DRL	MRL
0.00	370.17	0.80	259	370.50	0.84	252	370.27	0.88	244	370.18	0.91	239	370.38	0.95	226
0.05	210.15	0.46	148	196.09	0.46	133	184.08	0.46	119	177.16	0.46	112	164.10	0.45	97
0.10	127.92	0.28	90	112.64	0.26	76	101.14	0.25	65	94.91	0.25	59	83.71	0.23	49
0.25	42.24	0.09	31	33.29	0.08	23	27.94	0.07	18	25.57	0.07	17	21.82	0.06	12
0.50	14.25	0.02	11	10.40	0.02	8	8.82	0.02	6	8.22	0.02	5	7.16	0.02	3
0.75	7.76	0.01	6	5.55	0.01	4	4.83	0.01	3	4.51	0.01	3	3.79	0.01	2
1.00	5.26	0.01	5	3.77	0.01	3	3.28	0.01	2	3.02	0.01	2	2.39	0.01	2
1.50	3.34	0.00	3	2.36	0.00	2	1.98	0.00	1	1.82	0.00	1	1.22	0.00	1
2.00	2.65	0.00	2	1.77	0.00	1	1.47	0.00	1	1.38	0.00	1	0.72	0.00	0
3.00	2.20	0.00	2	1.27	0.00	1	1.12	0.00	1	1.11	0.00	1	0.26	0.00	0
4.00	2.07	0.00	2	1.10	0.00	1	1.04	0.00	1	1.04	0.00	1	0.10	0.00	0

Table 9. The ARL_1 performance of the MEDM-Sign control chart under the *Exponential*(1) distribution by varying $w = \{2, 5, 8, 10, 15\}$ and given $ARL_0 = 370$, $\lambda = 0.25$, and $n = 10$.

Shift	$(w, L) = (2, 8.655)$			$(w, L) = (5, 19.328)$			$(w, L) = (8, 28.737)$			$(w, L) = (10, 34.585)$			$(w, L) = (15, 48.279)$		
	ARL	S-DRL	MRL	ARL	S-DRL	MRL	ARL	S-DRL	MRL	ARL	S-DRL	MRL	ARL	S-DRL	MRL
0.00	370.20	0.80	259	370.35	0.84	253	370.41	0.88	246	370.72	0.89	242	370.47	0.94	231
0.05	168.79	0.37	118.5	154.07	0.07	105	141.16	0.35	92	134.59	0.34	86	121.41	0.33	73
0.10	88.16	0.19	63	75.03	0.17	52	65.22	0.16	43	60.60	0.15	39	52.17	0.14	32
0.25	23.42	0.04	18	17.96	0.04	13	15.04	0.03	11	13.92	0.03	9	12.12	0.03	6
0.50	7.73	0.01	7	5.72	0.01	5	5.03	0.01	3	4.71	0.01	3	4.05	0.01	2
0.75	4.30	0.01	4	3.29	0.01	3	2.86	0.01	2	2.62	0.01	2	2.17	0.01	2
1.00	2.97	0.00	3	2.31	0.00	2	1.93	0.00	1	1.73	0.00	1	1.41	0.00	1
1.50	1.91	0.00	2	1.46	0.00	1	1.13	0.00	1	0.94	0.00	1	0.75	0.00	1
2.00	1.50	0.00	1	1.16	0.00	1	0.75	0.00	1	0.55	0.00	0	0.45	0.00	0
3.00	1.18	0.00	1	1.02	0.00	1	0.32	0.00	1	0.20	0.00	0	0.17	0.00	0
4.00	1.07	0.00	1	1.00	0.00	1	0.13	0.00	0	0.07	0.00	0	0.07	0.00	0

Table 10. The ARL_1 performance of the MEDM–sign control chart under the *Exponential*(1) distribution by varying $w = \{2, 5, 8, 10, 15\}$ and given $ARL_0 = 370$, $\lambda = 0.25$, and $n = 15$.

Shift	$(w, L) = (2, 9.678)$			$(w, L) = (5, 21.835)$			$(w, L) = (8, 32.721)$			$(w, L) = (10, 39.545)$			$(w, L) = (15, 55.709)$		
	ARL	S-DRL	MRL	ARL	S-DRL	MRL	ARL	S-DRL	MRL	ARL	S-DRL	MRL	ARL	S-DRL	MRL
0.00	370.55	0.80	261	370.48	0.83	256	370.02	0.87	247	370.20	0.89	243	370.63	0.93	233
0.05	143.68	0.31	101	128.72	0.29	88	116.26	0.28	76	109.46	0.28	70	97.56	0.26	59
0.10	67.91	0.14	49	56.51	0.13	39	48.31	0.12	32	44.42	0.11	28	38.09	0.10	24
0.25	16.53	0.03	13	12.44	0.02	10	10.52	0.02	8	9.82	0.02	6	8.70	0.02	5
0.50	5.57	0.01	5	4.23	0.01	3	3.77	0.01	3	3.53	0.01	3	3.00	0.01	2
0.75	3.18	0.00	3	2.52	0.00	2	2.17	0.00	2	2.00	0.00	2	1.61	0.00	1
1.00	2.22	0.00	2	1.76	0.00	0	1.47	0.00	1	1.34	0.00	1	0.99	0.00	1
1.50	1.43	0.00	1	1.03	0.00	1	0.85	0.00	1	0.72	0.00	1	0.41	0.00	0
2.00	1.14	0.00	1	0.66	0.00	1	0.56	0.00	1	0.38	0.00	1	0.18	0.00	0
3.00	1.01	0.00	1	0.27	0.00	0	0.24	0.00	0	0.08	0.00	0	0.03	0.00	0
4.00	1.00	0.00	1	0.10	0.00	0	0.10	0.00	0	0.01	0.00	0	0.00	0.00	0

Table 11. The ARL_1 performance of the MEDM-Sign control chart under the *Gamma*(4, 1) distribution by varying $w = \{2, 5, 8, 10, 15\}$ and given $ARL_0 = 370$, $\lambda = 0.25$, and $n = 5$.

Shift	$(w, L) = (2, 5.934)$			$(w, L) = (5, 12.530)$			$(w, L) = (8, 17.819)$			$(w, L) = (10, 20.899)$			$(w, L) = (15, 27.726)$		
	ARL	S-DRL	MRL	ARL	S-DRL	MRL	ARL	S-DRL	MRL	ARL	S-DRL	MRL	ARL	S-DRL	MRL
0.00	370.09	0.81	259	370.22	0.87	249	370.11	0.92	238	370.11	0.94	230	370.26	1.00	209
0.05	268.26	0.59	188	256.60	0.62	171	248.36	0.64	156	242.65	0.64	147	232.07	0.66	127
0.10	197.53	0.44	138	181.69	0.44	120	170.08	0.44	106	163.02	0.44	98	149.87	0.43	81
0.25	86.25	0.19	61	72.55	0.18	48	63.51	0.17	40	58.82	0.16	35	50.62	0.15	28
0.50	29.49	0.06	21	22.74	0.05	15	19.15	0.05	13	17.60	0.05	11	15.09	0.04	6
0.75	13.50	0.03	10	10.01	0.02	7	8.46	0.02	5	7.87	0.02	4	6.86	0.02	2
1.00	7.52	0.01	6	5.54	0.01	4	4.68	0.01	2	4.35	0.01	2	3.73	0.01	1
1.50	3.28	0.01	3	2.44	0.01	2	1.85	0.01	1	1.66	0.01	1	1.36	0.01	1
2.00	1.88	0.00	1	1.28	0.00	1	0.77	0.00	0	0.67	0.00	0	0.57	0.00	0
3.00	1.11	0.00	01	0.27	0.00	0	0.12	0.00	0	0.10	0.00	0	0.09	0.00	0
4.00	1.00	0.00	1	0.00	0.00	0	0.00	0.00	0	0.00	0.00	0	0.00	0.00	0

Table 12. The ARL_1 performance of the MEDM–sign control chart under the *Gamma*(4, 1) distribution by varying $w = \{2, 5, 8, 10, 15\}$ and given $ARL_0 = 370$, $\lambda = 0.25$, and $n = 10$.

Shift	$(w, L) = (2, 6.641)$			$(w, L) = (5, 14.195)$			$(w, L) = (8, 20.413)$			$(w, L) = (10, 24.115)$			$(w, L) = (15, 32.485)$		
	ARL	S-DRL	MRL	ARL	S-DRL	MRL	ARL	S-DRL	MRL	ARL	S-DRL	MRL	ARL	S-DRL	MRL
0.00	370.25	0.80	260	370.44	0.86	251	370.33	0.90	242	370.03	0.92	236	370.56	0.97	221
0.05	263.73	0.52	165	223.79	0.53	150	212.38	0.53	137	205.68	0.53	129	193.71	0.53	112
0.10	154.44	0.34	108	138.50	0.33	93	126.12	0.32	80	120.05	0.32	74	107.91	0.30	61
0.25	53.34	0.11	38	43.01	0.10	29	36.81	0.09	24	33.87	0.09	21	28.95	0.08	17
0.50	15.41	0.03	12	11.58	0.03	9	9.88	0.02	6	9.19	0.02	5	8.03	0.02	3
0.75	6.83	0.01	6	5.11	0.01	4	4.42	0.01	3	4.13	0.01	2	3.45	0.01	2
1.00	3.79	0.01	3	2.89	0.01	2	2.41	0.01	1	2.22	0.01	1	1.69	0.01	1
1.50	1.59	0.00	1	1.14	0.00	1	0.83	0.00	0	0.76	0.00	0	0.42	0.00	0
2.00	0.80	0.00	1	0.41	0.00	0	0.29	0.00	0	0.27	0.00	0	0.08	0.00	0
3.00	0.17	0.00	0	0.02	0.00	0	0.01	0.00	0	0.01	0.00	0	0.00	0.00	0
4.00	0.00	0.00	0	0.00	0.00	0	0.00	0.00	0	0.00	0.00	0	0.00	0.00	0

Table 13. The ARL_1 performance of the MEDM–sign control chart under the *Gamma*(4, 1) distribution by varying $w = \{2, 5, 8, 10, 15\}$ and given $ARL_0 = 370$, $\lambda = 0.25$, and $n = 15$.

Shift	$(w, L) = (2, 7.168)$			$(w, L) = (5, 15.456)$			$(w, L) = (8, 22.415)$			$(w, L) = (10, 26.615)$			$(w, L) = (15, 36.195)$		
	ARL	S-DRL	MRL	ARL	S-DRL	MRL	ARL	S-DRL	MRL	ARL	S-DRL	MRL	ARL	S-DRL	MRL
0.00	370.97	0.81	259	370.36	0.85	252	370.30	0.89	243	370.44	0.91	238	370.26	0.96	225
0.05	214.31	0.48	149	199.74	0.47	134	187.61	0.47	121	191.72	0.47	114	168.58	0.46	98
0.10	129.97	0.28	91	114.13	0.27	77	102.43	0.26	66	96.62	0.25	60	85.69	0.24	50
0.25	38.73	0.08	28	30.48	0.07	21	25.85	0.06	17	23.83	0.06	16	20.47	0.06	11
0.50	10.55	0.02	8	7.86	0.02	6	6.82	0.02	4	6.39	0.02	4	5.55	0.02	3
0.75	4.66	0.01	4	3.53	0.01	3	3.08	0.01	2	2.81	0.01	2	2.28	0.01	1
1.00	2.58	0.00	2	1.96	0.00	1	1.63	0.00	1	1.40	0.00	1	1.07	0.00	1
1.50	1.03	0.00	1	0.64	0.00	0	0.47	0.00	0	0.33	0.00	0	0.24	0.00	0
2.00	0.44	0.00	0	0.17	0.00	0	0.10	0.00	0	0.05	0.00	0	0.04	0.00	0
3.00	0.03	0.00	0	0.00	0.00	0	0.00	0.00	0	0.01	0.00	0	0.00	0.00	0
4.00	0.00	0.00	0	0.00	0.00	0	0.00	0.00	0	0.00	0.00	0	0.00	0.00	0

Table 14. The overall performance efficacy of the MEDM–sign control chart under various distributions by varying $w = \{2, 5, 8, 10, 15\}$, $n = \{5, 10, 15\}$, and $\lambda = 0.25$.

		AEQL			PCI			RMI		
		$n = 5$	$n = 10$	$n = 15$	$n = 5$	$n = 10$	$n = 15$	$n = 5$	$n = 10$	$n = 15$
	$w = 2$	1.42	0.58	0.34	2.56	2.46	2.34	4.61	1.97	2.94
	$w = 5$	1.03	0.42	0.25	1.86	1.76	1.73	2.35	1.03	1.32
$Normal(0, 1)$	$w = 8$	0.79	0.35	0.21	1.43	1.48	1.43	0.59	0.66	0.72
	$w = 10$	0.69	0.30	0.18	1.25	1.26	1.26	0.24	0.31	0.35
	$w = 15$	0.55	0.24	0.15	1.00	1.00	1.00	0.00	0.00	0.00
	$w = 2$	2.04	0.66	0.32	3.56	3.14	2.73	5.02	3.63	2.22
	$w = 5$	2.09	0.41	0.22	3.64	1.98	1.88	3.39	1.51	1.13
$Laplace(0, 1)$	$w = 8$	0.90	0.34	0.18	0.75	1.61	1.51	0.57	0.97	0.62
	$w = 10$	0.75	0.28	0.15	1.30	1.33	1.31	0.30	0.40	0.33
	$w = 15$	0.57	0.21	0.12	1.00	1.00	1.00	0.00	0.00	0.00
	$w = 2$	8.06	4.38	3.67	4.80	4.24	7.04	3.32	2.65	4.57
	$w = 5$	4.96	3.72	1.35	2.95	3.60	2.60	1.71	2.14	1.52
$Exponential(1)$	$w = 8$	4.41	1.57	1.18	2.62	1.52	2.27	1.44	0.41	1.19
	$w = 10$	4.26	1.22	0.79	2.53	1.18	1.52	1.37	0.15	0.47
	$w = 15$	1.68	1.03	0.52	1.00	1.00	1.00	0.00	0.00	0.00
	$w = 2$	6.49	2.30	1.60	3.14	2.46	2.51	1.92	1.84	2.27
	$w = 5$	3.35	1.61	1.05	1.62	1.72	1.65	0.62	0.93	0.86
$Gamma(4, 1)$	$w = 8$	2.62	1.33	0.88	1.27	1.42	1.38	0.23	0.56	0.46
	$w = 10$	2.40	1.23	0.77	1.16	1.32	1.20	0.13	0.46	0.19
	$w = 15$	2.07	0.93	0.64	1.00	1.00	1.00	0.00	0.00	0.00

Table 15. The performance of ARL_1 and MRL for the MEDM–sign control charts under the $Normal(0, 1)$ distribution with $w = 5$, $\lambda = 0.25$, $n = 5$, and $ARL_0 = 370$.

Shift	Shewhart		EWMA		MA		DMA		MEM		MEDM		MEDM-SN	
	$L = 3.000$		$L_1 = 2.927$		$L_2 = 2.884$		$L_3 = 5.235$		$L_4 = 6.480$		$L_5 = 9.997$		$L_7 = 9.935$	
	ARL	MRL	ARL	MRL	ARL	MRL	ARL	MRL	ARL	MRL	ARL	MRL	ARL	MRL
−4.00	1.19	1	1.08	1	1.00	1	0.00	**0**	1.02	1	0.17	**0**	**0.00**	**0**
−3.00	2.00	1	1.38	1	1.10	1	0.03	**0**	1.27	1	0.60	1	**0.01**	**0**
−2.00	6.34	5	2.51	2	1.99	2	0.45	**0**	2.47	2	1.63	1	**0.12**	**0**
−1.50	14.98	11	4.19	4	3.76	3	1.44	**0**	4.19	4	2.86	2	**0.41**	**0**
−1.00	43.83	30	9.09	7	10.17	7	5.06	**0**	9.26	7	6.24	4	**1.40**	1
−0.75	81.05	56	16.72	13	20.61	15	11.42	8	17.00	15	11.39	5	**2.82**	**1**
−0.50	155.20	107	39.93	29	51.62	36	32.66	18	40.10	36	27.67	14	**7.18**	**5**
−0.25	281.36	196	136.26	96	162.27	113	126.01	67	134.98	113	104.87	57	**35.04**	**23**
−0.10	353.25	245.5	307.28	217	311.20	216	289.66	173	294.27	216	272.19	135	**167.70**	**106**
−0.05	366.04	255	351.09	260	353.55	246	345.01	216	347.11	246	340.65	**161**	**287.86**	183
0.00	370.00	257	370.00	285	370.36	258	370.01	243	370.32	257	370.72	234	370.02	236
0.05	365.82	255	344.66	263	354.09	246	343.88	215	346.89	246	339.64	**161**	**288.66**	183
0.10	353.03	245	302.15	226	311.23	216	287.02	171	293.07	216	269.78	134	**167.70**	**106**
0.25	281.60	196	138.84	98	162.75	113	125.49	67	134.23	112	104.49	57	**34.98**	**22**
0.50	155.23	107	40.76	29	51.64	36	32.54	18	39.99	36	27.49	14	**7.15**	**5**
0.75	81.23	56	16.70	12	20.58	15	11.36	8	16.92	13	11.33	5	**2.80**	**1**
1.00	43.92	31	9.11	7	10.13	7	5.01	**0**	9.21	7	6.21	4	**1.38**	1
1.50	14.99	11	4.18	4	3.76	3	1.43	**0**	4.18	4	2.85	2	**0.40**	**0**
2.00	6.33	5	2.54	2	1.99	2	0.45	**0**	2.48	2	1.63	1	**0.12**	**0**
3.00	2.00	2	1.39	1	1.10	1	0.03	**0**	1.27	1	0.60	1	**0.01**	**0**
4.00	1.19	1	1.08	1	1.00	1	**0.00**	**0**	1.02	1	0.17	**0**	**0.00**	**0**
AEQL	23.9384		7.6927		7.9069		3.8415		7.5526		5.0481		**1.1399**	
PCI	21.0008		6.7487		6.9366		3.3701		6.6258		4.4286		**1.0000**	
RMI	39.4019		19.5741		16.4665		2.1079		18.3188		9.4517		**0.0000**	

Note: The bold is the minimum of ARL and MRL.

Table 16. The performance of ARL_1 and MRL for the MEDM–sign control charts under the $Laplace(0, 1)$ distribution with $w = 5$, $\lambda = 0.25$, $n = 5$, and $ARL_0 = 370$.

Shift	Shewhart		EWMA		MA		DMA		MEM		MEDM		MEDM-SN	
	$L = 3.112$		$L_1 = 3.396$		$L_2 = 3.112$		$L_3 = 4.010$		$L_4 = 7.455$		$L_5 = 7.411$		$L_7 = 9.930$	
	ARL	MRL	ARL	MRL	ARL	MRL	ARL	MRL	ARL	MRL	ARL	MRL	ARL	MRL
−4.00	13.57	10	1.79	2	1.20	1	0.08	**0**	1.67	2	0.85	1	**0.05**	**0**
−3.00	36.78	26	2.93	9	1.98	2	0.32	**0**	2.82	3	1.49	1	**0.13**	**0**
−2.00	98.16	68	6.88	17	5.37	4	1.73	**0**	6.59	6	3.29	2	**0.41**	**0**
−1.50	157.19	109	14.01	53	12.59	9	5.58	1	13.33	11	5.93	4	**0.79**	**0**
−1.00	239.88	167	38.94	84	38.69	27	22.35	12	36.68	27	15.39	11	**1.78**	**1**
−0.75	286.24	199	74.36	111	74.40	52	48.62	26	69.53	49	30.82	21	**3.06**	**1**
−0.50	328.52	228	159.05	132	147.66	102	111.84	63	139.76	98	74.06	49	**6.64**	**4**
−0.25	359.02	249	287.64	176	277.65	191	247.47	143	270.37	188	200.71	131	**27.05**	**18**
−0.10	368.91	256	357.64	228	352.11	243	341.63	214	349.75	243	328.39	198	**133.36**	**84**
−0.05	370.11	257	365.47	251	365.43	253	360.82	234	364.94	254	358.50	208	**259.02**	**164**
0.00	370.80	257	370.42	259	370.36	256	369.56	256	370.56	257	370.04	241	370.28	236
0.05	370.46	257	362.05	252	364.71	253	361.31	233	364.98	253	358.15	209	**258.28**	**164**
0.10	368.83	255	349.88	229	351.64	244	342.47	213	349.78	243	327.91	198	**133.26**	**84**
0.25	358.55	249	283.41	178	276.56	192	246.67	142	270.17	188	201.32	131	**27.11**	**18**
0.50	328.30	227	150.03	134	147.88	102	111.19	62	138.99	97	73.96	49	**6.64**	**4**
0.75	285.57	198	72.00	109	74.46	52	48.55	26	69.24	49	30.94	21	**3.06**	**1**
1.00	239.35	166	38.23	87	38.79	27	22.39	12	36.77	27	15.37	11	**1.79**	**1**
1.50	156.62	109	13.95	49	12.52	9	5.56	1	13.38	11	5.94	4	**0.79**	**0**
2.00	97.90	68	6.69	16	5.35	4	1.72	**0**	6.60	6	3.28	2	**0.41**	**0**
3.00	36.71	26	2.88	8	1.98	2	0.32	**0**	2.83	3	1.49	1	**0.13**	**0**
4.00	13.52	10	1.77	4	1.20	1	0.08	**0**	1.67	2	0.85	1	**0.05**	**0**
AEQL	166.8883		23.7280		21.7693		12.5953		22.5004		9.0635		**1.4133**	
PCI	118.0875		16.7896		15.4036		8.9122		15.9209		6.4132		**1.0000**	
RMI	105.8891		13.7897		12.3961		6.6325		13.0502		6.2222		**0.0001**	

Note: The bold is the minimum of ARL and MRL.

Table 17. The performance of ARL_1 and MRL for the MEDM–sign control chart under the *Exponential*(1) distribution with $w = 5$, $\lambda = 0.25$, $n = 5$, and $ARL_0 = 370$.

Shift	Shewhart		EWMA		MA		DMA		MEM		MEDM		MEDM-SN	
	$L = 4.915$		$L_1 = 3.747$		$L_2 = 3.339$		$L_3 = 5.950$		$L_4 = 8.251$		$L_5 = 11.750$		$L_7 = 16.015$	
	ARL	MRL	ARL	MRL	ARL	MRL	ARL	MRL	ARL	MRL	ARL	MRL	ARL	MRL
0.00	370.11	256	370.00	278	370.82	257	370.74	241	370.30	258	370.01	119	370.50	252
0.05	279.28	193	269.58	191	253.40	175	243.81	156	253.18	178	233.24	**79**	**196.09**	133
0.10	216.01	150	193.54	139.5	180.02	124	169.96	108	180.74	127	155.38	**55**	**112.64**	76
0.25	113.40	78	85.31	60	78.99	54	71.05	44	81.21	58	61.22	25	**33.29**	**23**
0.50	51.52	36	33.55	25	31.40	22	26.36	16	33.76	25	22.95	11	**10.40**	**8**
0.75	29.33	20	19.49	15	17.01	12	13.80	8	19.41	15	12.77	7	**5.55**	**4**
1.00	19.25	13	13.15	10	10.95	8	8.69	5	13.18	10	8.71	6	**3.77**	**3**
1.50	10.63	8	8.12	6	6.09	4	4.38	**2**	7.86	6	5.42	4	**2.36**	**2**
2.00	7.18	5	5.70	5	4.15	3	2.44	**1**	5.60	5	4.04	3	**1.77**	**1**
3.00	4.38	3	3.82	3	2.59	2	**0.90**	**0**	3.60	3	2.76	2	1.27	1
4.00	3.26	2	3.01	2	1.97	1	**0.46**	**0**	2.72	2	2.11	1	1.10	1
AEQL	18.4356		14.9138		10.9883		5.8970		14.1872		10.4135		**4.9645**	
PCI	3.7135		3.0041		2.2134		1.1878		2.8578		2.0976		**1.0000**	
RMI	2.9643		2.1209		1.4854		0.6772		1.9984		1.2235		**0.1640**	

Note: The bold is the minimum of ARL and MRL.

Table 18. The performance of ARL_1 and MRL for the MEDM–sign control chart under the $Gamma(4, 1)$ distribution with $w = 5$, $\lambda = 0.25$, $n = 5$, and $ARL_0 = 370$.

Shift	Shewhart		EWMA		MA		DMA		MEM		MEDM		MEDM-SN	
	$L = 3.894$		$L_1 = 3.549$		$L_2 = 3.023$		$L_3 = 2.731$		$L_4 = 7.600$		$L_5 = 7.415$		$L_7 = 12.530$	
	ARL	MRL	ARL	MRL	ARL	MRL	ARL	MRL	ARL	MRL	ARL	MRL	ARL	MRL
0.00	370.18	257	370.04	193	370.52	258	370.04	199	370.60	194	370.18	178	370.22	249
0.05	325.07	226	311.13	182.5	283.92	197	273.40	172	286.90	147	**248.86**	**117**	256.60	133
0.10	287.04	199	247.13	165	219.56	152	289.68	147	224.43	117	214.90	**71**	**181.69**	120
0.25	198.65	137	145.89	71	108.91	76	147.56	96	114.93	70	142.43	54	**72.55**	**48**
0.50	113.45	79	53.20	42	41.48	29	52.14	49	47.17	33	48.07	27	**22.74**	**15**
0.75	68.21	47	25.79	29	19.52	14	23.00	27	24.76	19	21.45	13	**10.01**	**7**
1.00	43.06	30	16.17	18	10.75	8	9.52	7	15.65	13	18.49	9	**5.54**	**4**
1.50	19.44	14	8.50	9	4.53	3	3.96	**2**	8.49	8	7.37	5	**2.44**	**2**
2.00	10.10	7	5.87	5	2.53	2	2.01	2	5.74	5	4.18	2	**1.28**	**1**
3.00	3.81	3	3.49	2	1.32	1	1.29	**0**	3.41	3	2.62	1	**0.27**	**0**
4.00	2.06	2	2.46	1	1.06	1	0.93	**0**	2.37	2	2.43	1	**0.00**	**0**
AEQL	25.2072		15.4290		8.2695		8.3396		14.7443		13.6372		**3.3535**	
PCI	7.5167		4.6009		2.4660		2.4868		4.3967		4.0666		**1.0000**	
RMI	5.1299		2.7168		1.0319		1.1119		2.5487		2.0811		**0.0035**	

Note: The bold is the minimum of ARL and MRL.

5. Comparative results

In this section, we compare the performance of the MEDM–sign control chart with some existing control charts, including the Shewhart, EWMA, MA, DMA, and MEDM control charts, using the ARL, S-DRL, and MRL criteria to analyze changes of a specific magnitude. These metrics help evidence-based parameter selection in practical applications by allowing a thorough assessment of each parameter combination's stability and sensitivity for anomaly identification. Additionally, the overall performance of the MEDM–sign control chart is calculated by applying the AEQL, PCI, and RMI criteria to compare it with some existing control charts. All control charts are proposed using $ARL_0 = 370$, $n = 5$, $w = 5$, and $\lambda = 0.25$, with their corresponding framework parameters for a logical comparison. Tables 15–18 demonstrate the numerical results using the *Normal*(0, 1), *Laplace*(0, 1), *Exponential*(1), and *Gamma*(4, 1) distributions, respectively.

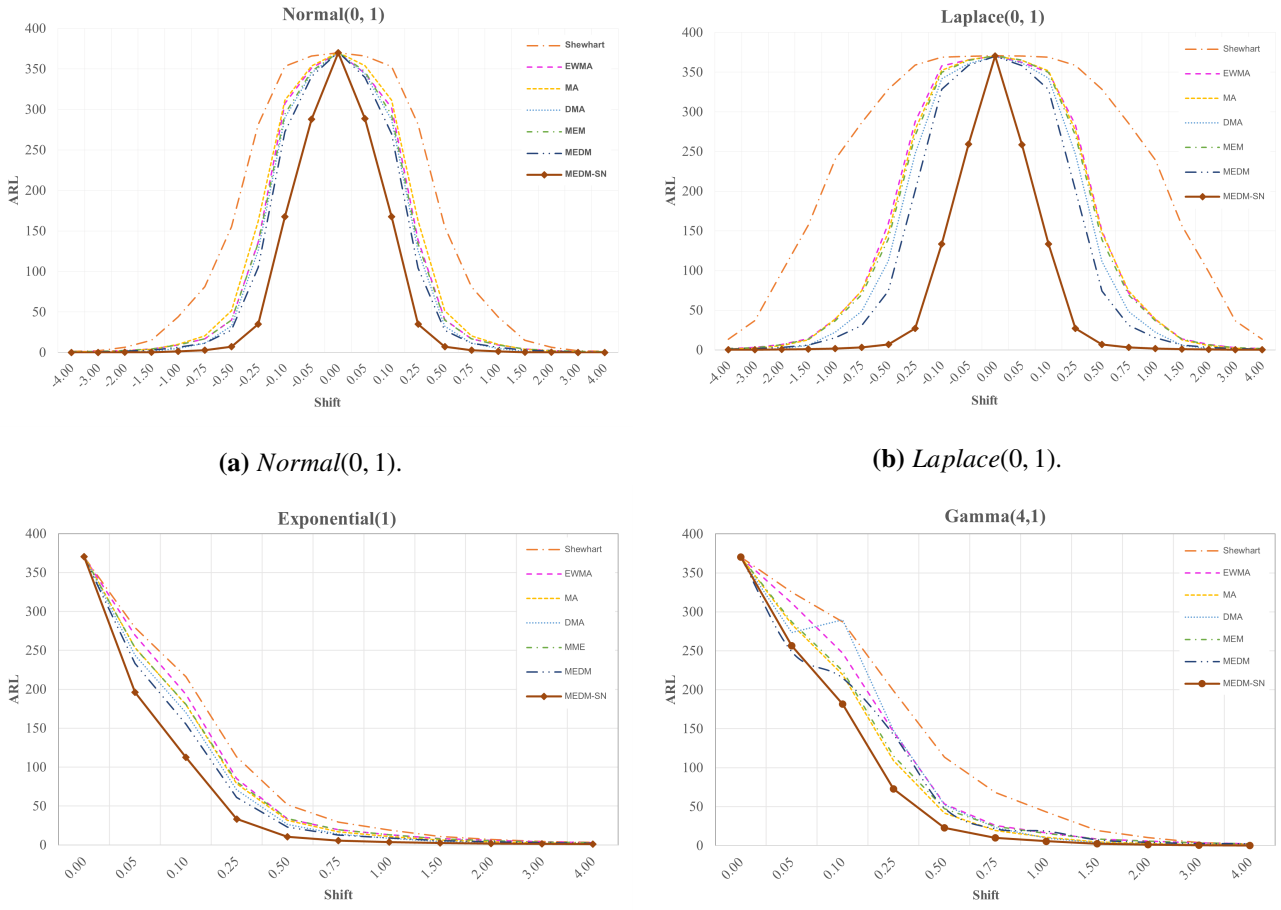

(a) *Normal*(0, 1).

(b) *Laplace*(0, 1).

(c) *Exponential*(1).

(d) *Gamma*(4, 1).

Figure 1. The ARL shapes of the EWMA, MA, DMA, MEM, MEDM, and MEDM–sign control charts at $ARL_0 = 370$, $w = 5$, $\lambda = 0.25$, and $n = 5$ under different distributions.

The MEDM–sign control chart yields the following intriguing results. Under the *Normal*(0, 1) and *Laplace*(0, 1) distributions, we found that the MEDM–sign control chart has minimal ARL_1 values

as compared with the existing control charts, as shown in Tables 15 and 16 and Figure 1a, 1b. The MEDM–sign control chart has minimal ARL_1 values except for shifts of $\delta > 2.00$, whereas the MEDM control chart works somewhat better under the *Exponential*(1) distribution, as shown in Table 17 and Figure 1c. Similarly, in the case of the *Gamma*(4, 1) distribution, the MEDM–sign control chart has minimal ARL_1 values except for $\delta < 0.10$, as shown in Table 18 and Figure 1d. Furthermore, the numerical results from Tables 15–18 show that the MEDM–sign control chart has lower AEQL, PCI, and RMI values than its rivals, demonstrating its overall superior shift capability. In addition, if we compare the GWMA-based charts, including the GWMA–sign and GWMA–signed–rank charts, with the MEDM–sign chart, then the proposed chart uses a dual smoothing approach that combines the EWMA and DMA charts with sign statistics. This chart increases the sensitivity to small changes while maintaining simplicity in its interpretation and parameter usage. It can be seen that the proposed chart differs from the GWMA-based charts, which require specifying multiple weight parameters. Therefore, the proposed chart uses fewer parameters and is easier to understand, making it more suitable for practical use. A deeply detailed numerical comparative result with the GWMA–sign and GWMA–signed–rank charts is ignored in this paper but not in future research.

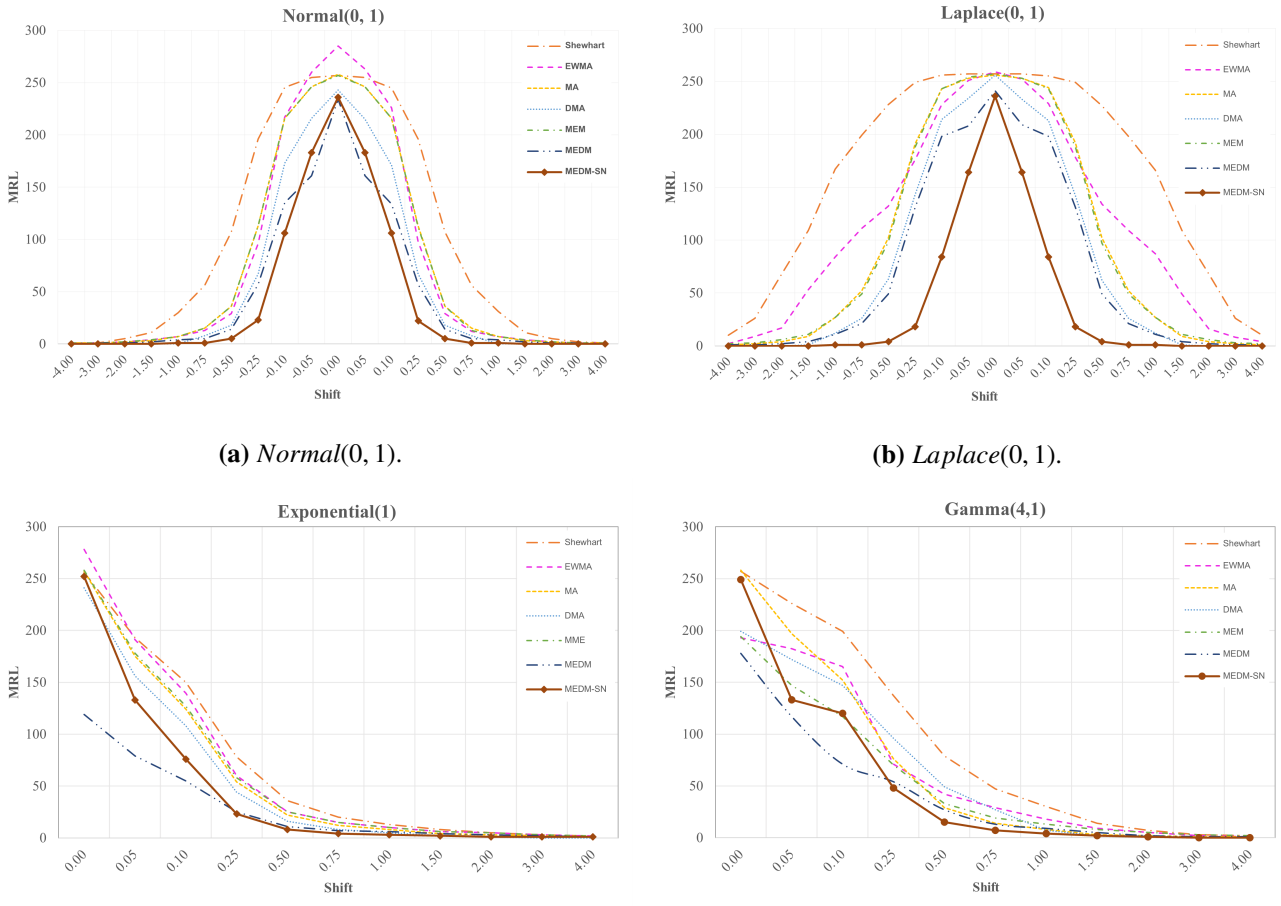

(a) *Normal*(0, 1).

(b) *Laplace*(0, 1).

(c) *Exponential*(1).

(d) *Gamma*(4, 1).

Figure 2. The *MRL* shapes of the EWMA, MA, DMA, MEM, MEDM, and MEDM–sign control charts at $ARL_0 = 370$, $w = 5$, $\lambda = 0.25$, and $n = 5$ under different distributions.

6. Applications to real data sets

This section applies the proposed control chart to three datasets and discusses their usefulness. We have focused on three applications: (i) The die-casting hot chamber process is used in manufacturing zinc alloy (ZAMAK) parts for the sanitary industry [38], (ii) the survival times of a cluster of patients suffering from head and neck cancer disease who were treated with radiotherapy (RT) [39], and (iii) the measurements of the outer diameter at base of stem of an exhaust valve bridge [40].

6.1. The die-casting hot chamber process used in manufacturing ZAMAK parts for the sanitary industry

This dataset presents the die-casting hot chamber process used in manufacturing ZAMAK parts for the sanitary industry [38]. The dataset is given as follows: 292.6, 289.0, 291.4, 288.0, 290.0, 288.2, 535.4, 518.4, 529.2, 527.0, 533.6, 439.2, 447.2, 443.4, 434.0, 436.0, 437.6, 419.6, 422.4, 416.8, 420.4, 421.6, 418.4, 410.4, 449.0, 441.6, 393.2, 401.8, and 412.6. This dataset presents a Phase *I* IC dataset of 30 samples of size $n = 5$. It was confirmed to have a normal distribution with parameter values with a mean of 420.31 and a standard deviation of 77.75863 (p-value = 0.2388 > 0.05) by the Kolmogorov–Smirnov test. Figure 3a, 3g show the simulation's performance results in detecting the mean of the die-casting hot chamber process used in manufacturing ZAMAK parts for the sanitary industry, applying the Shewhart, EWMA, MA, DMA, MEM, MEDM, and MEDM–sign control charts. Figure 3g illustrates that the mean shift process is identifiable at the first observation under the MEDM–sign control chart. As illustrated in Figure 3b, 3c, 3e, the EWMA, MA, and MEM control charts identify a change in the process's mean at the fourth observation. Finally, the Shewhart, DMA, and MEDM control charts failed to identify a change in the process's mean at any observation value, as illustrated in Figure 3a, 3d, 3f. As a result, we conclude that the MEDM–sign control chart is more effective than other control charts in detecting changes in the process's mean.

6.2. The survival times of a cluster of patients suffering from head and neck cancer disease who were treated with RT

This dataset displays the survival times of a cluster of patients suffering from head and neck cancer disease who were treated with RT [39]. The dataset is as follows: 6.53, 7, 10.42, 14.48, 16.1, 22.7, 34, 41.55, 42, 45.28, 49.4, 53.62, 63, 64, 83, 84, 91, 108, 112, 129, 133, 133, 139, 140, 140, 146, 149, 153, 157, 160, 160, 165, 146, 149, 154, 157, 160, 160, 165, 173, 176, 218, 225, 241, 248, 273, 277, 297, 405, 417, 420, 440, 523, 583, 594, 1101, 1146, and 1417. This dataset was confirmed to have an asymptotic exponential distribution with parameter values with a rate of 0.0044217158 (p-value = 0.08143 > 0.05) by the Kolmogorov–Smirnov test. Figure 4a–4g) displays the simulation's performance results in detecting the mean survival times of a cluster of patients suffering from head and neck cancer disease and treated using RT, applying the Shewhart, EWMA, MA, DMA, MEM, MEDM, and MEDM–sign control charts. Figure 4g illustrates that the mean shift of the process is identifiable at the first observation with the MEDM–sign control chart. As illustrated in Figure 4b, 4c, the EWMA and MA control charts identify a change in the process's mean at the 56^{th} observation. Figure 4e shows that the mean shift of the process is identifiable at the 58^{th} observation with the MEM control chart. Finally, the Shewhart, DMA, and MEDM control charts failed to identify a change in the process's mean at any observation value, as illustrated in Figure 4a, 4d, 4f. As a result, we conclude that the MEDM–sign control chart is more effective than other control charts in detecting changes in

the process's mean.

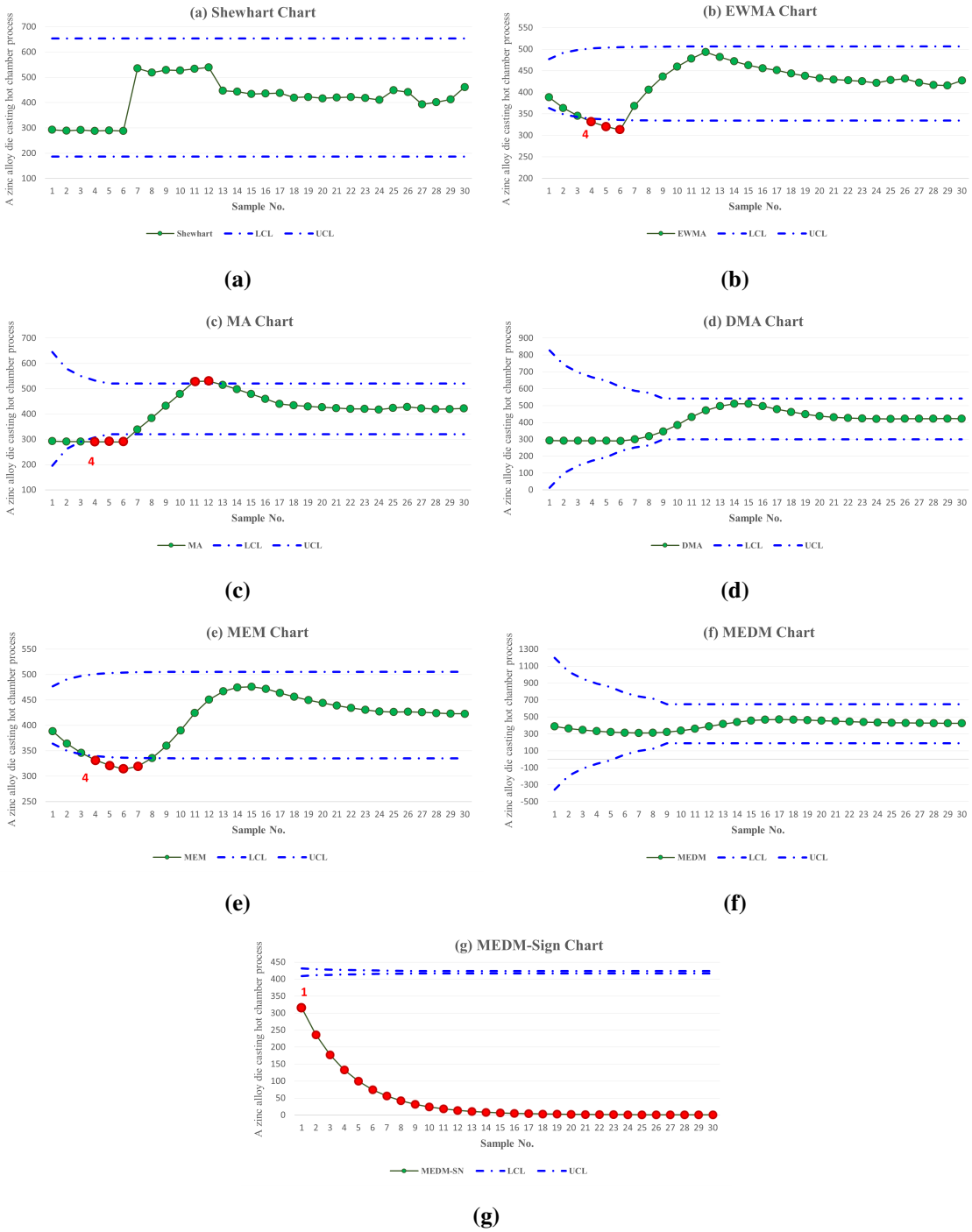

Figure 3. Simulation performance results of the dataset of die-casting hot chamber process used in manufacturing ZAMAK parts for the sanitary industry of the existing control charts: (a) Shewhart; (b) EWMA; (c) MA; (d) DMA; (e) MEM; (f) MEDM; (g) MEDM–sign.

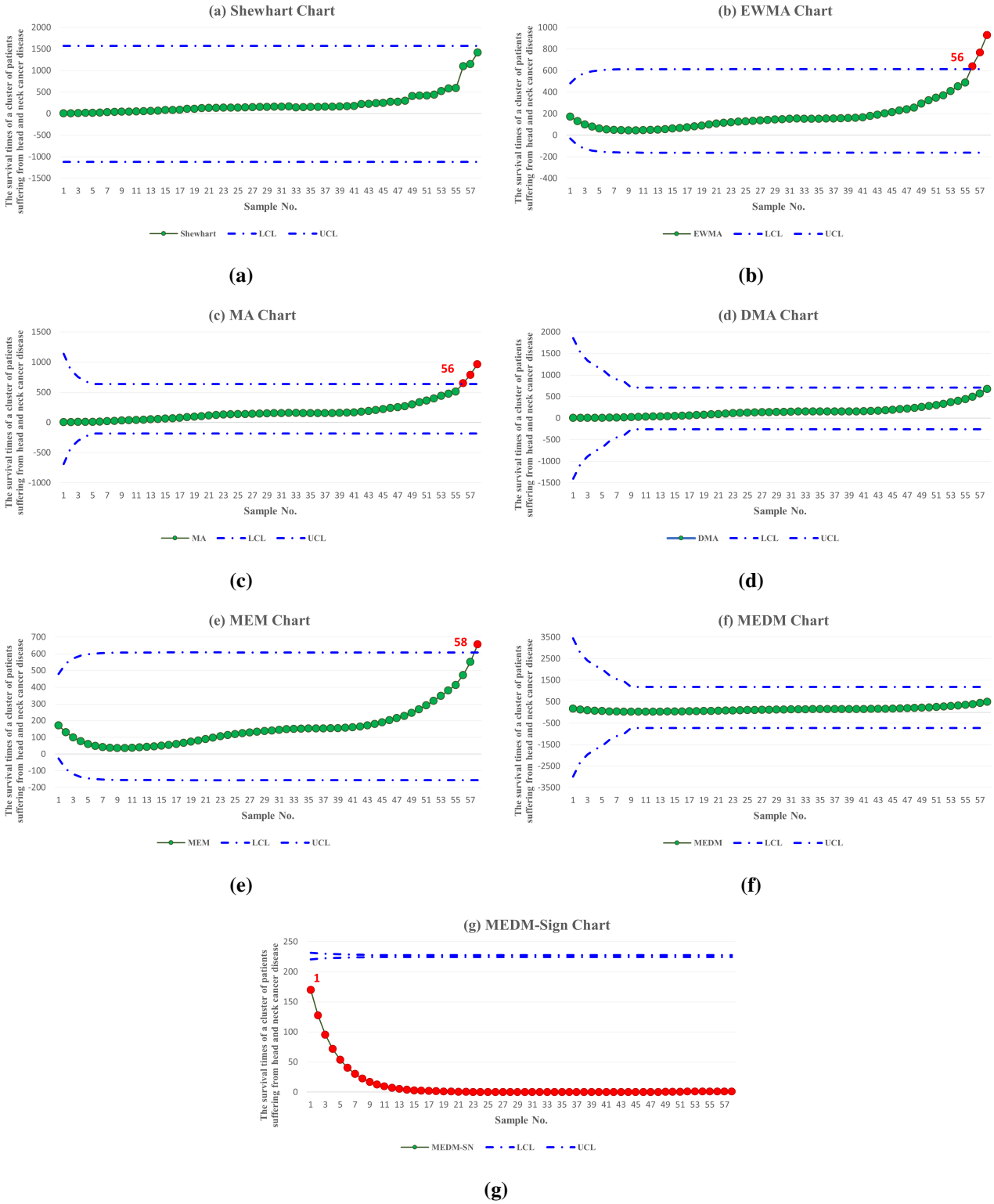

Figure 4. Simulation performance results of the dataset of survival times of a cluster of patients suffering from head and neck cancer disease who were treated with RT of the existing control charts: (a) Shewhart; (b) EWMA; (c) MA; (d) DMA; (e) MEM; (f) MEDM; (g) MEDM–sign.

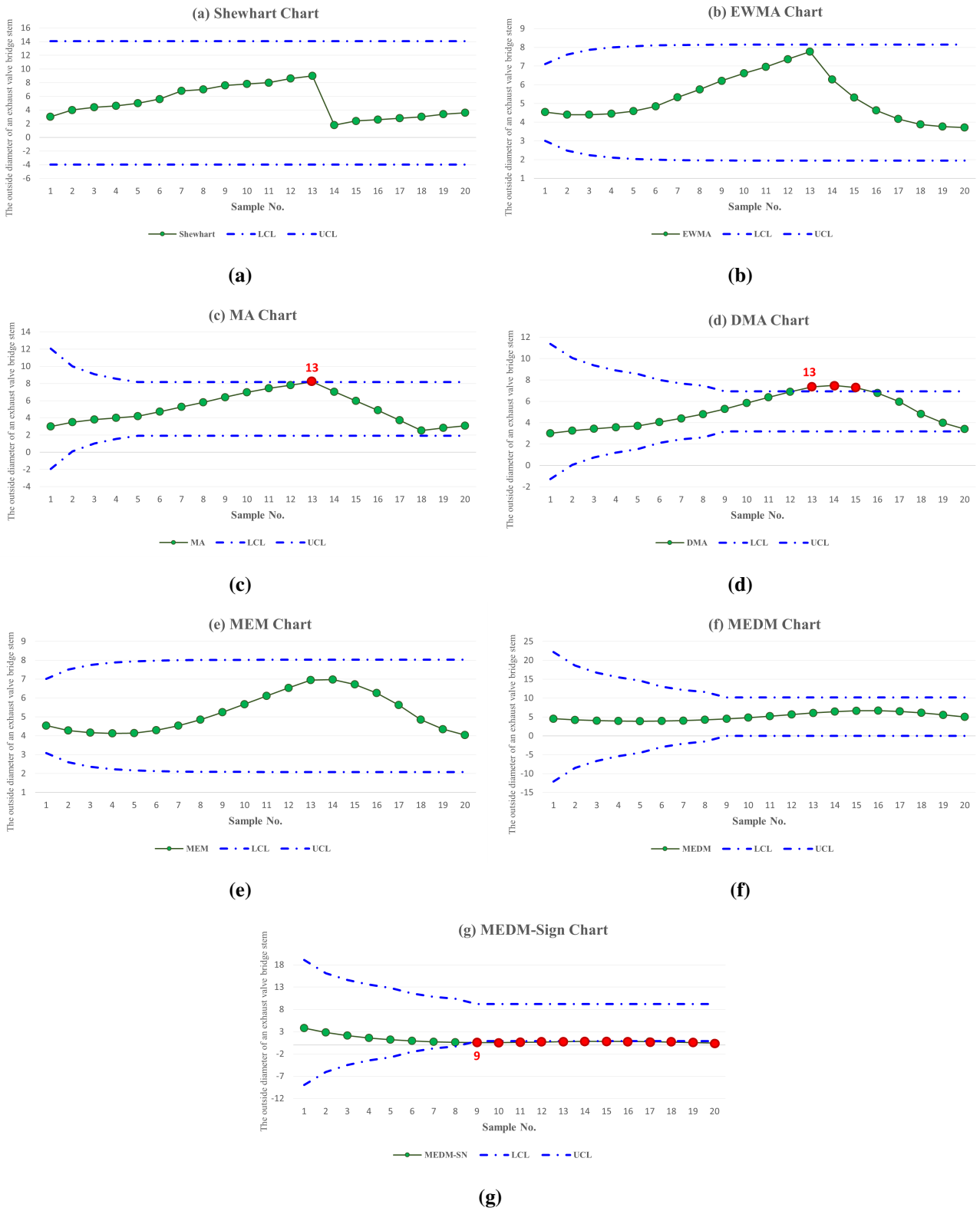

Figure 5. Simulation performance results of the dataset of measurements of the outer diameter at the base of the stem of an exhaust valve bridge of the existing control charts: (a) Shewhart; (b) EWMA; (c) MA; (d) DMA; (e) MEM; (f) MEDM; (g) MEDM–sign.

6.3. The measurements of the outer diameter at the base of the stem of an exhaust valve bridge

This case study relates to controlling the outside diameter of an exhaust valve bridge stem, with a required particular of 1.1550–1.1560 inches [40]. The data set consists of 20 samples, each with a size of $n = 5$, and each sample is 0.0001 inches above 1.1550 inches. The dataset is as follows: 3.0, 4.0, 4.4, 4.6, 5.0, 5.6, 6.8, 7.0, 7.6, 7.8, 8.0, 8.6, 9.0, 1.8, 2.4, 2.6, 2.8, 3.0, 3.4, and 3.6. This dataset was confirmed to have an asymptotic gamma distribution with parameter values with a shape of 4.8382765 and a scale of 0.9580745 (p-value = 0.7685 > 0.05) by the Kolmogorov–Smirnov test. Figure 5a–5g display the simulation's performance results in detecting the mean of the outside diameter of an exhaust valve bridge stem, applying the Shewhart, EWMA, MA, DMA, MEM, MEDM, and MEDM–sign control charts. Figure 5g illustrates that the mean shift of the process is identifiable at the ninth observation under the MEDM–sign control chart. As illustrated in Figure 5c, 5d, the MA and DMA control charts identify a change in the process's mean at the 13^{th} observation, respectively. Finally, the Shewhart, EWMA, MEM, and MEDM control charts failed to identify a change in the process's mean at any observation value, as illustrated in Figure 5a, 5b, 5e, 5f. As a result, we conclude that the MEDM–sign control chart is more effective than other control charts in detecting changes in the process's mean.

7. Conclusions

Non-parametric control charts are a dependable and useful tool for assessing a process when the real distribution of the quality attributes is unknown. To detect changes in the process's mean, we developed a mixed control chart with no distribution and employed the sign statistic (MEDM–sign chart). MC simulations with both symmetric and asymmetric distributions are used to assess how the efficacy control charts that use the minimum ARL_1 work. Nonetheless, the overall performance criteria based on the AEQL, PCI, and RMI values indicated that the MEDM-Sign chart outperformed the others throughout the whole range of shifts in all distributions. The results demonstrated that the MEDM–sign chart detects various changes more effectively than other charts. Three real-life examples are also offered to demonstrate how the proposed chart differs from earlier control charts in terms of usefulness and capacity to identify process modifications. Additionally, this analysis can be applied to data with both symmetric and asymmetric distributions. According to our results, the MEDM–sign control chart is an alternative to a nonparametric control chart. In future work, we plan to develop new control chart formulations based on nonparametric statistics and to investigate processes governed by alternative distributional structures. Although the present study does not include comparisons with the GWMA–sign and GWMA–signed–rank charts, these methods constitute important nonparametric benchmarks, and incorporating such comparisons will form a valuable extension of our subsequent research and provide a complete picture of the performance of the proposed chart.

Author contributions

Weerawat Sudsutad: Software, formal analysis, investigation, data curation, writing—original draft preparation; Yupaporn Areepong: Validation, visualization; Saowanit Sukparungsee: Conceptualization, methodology, writing—review and editing, visualization, project administration. All authors have read and agreed to the published version of the manuscript.

Use of Generative-AI tools declaration

The authors declare that they have not used Artificial Intelligence (AI) tools in the creation of this article.

Acknowledgments

All authors would like to thank the Department of Applied Statistics for its assistance and the use of the supercomputer. Furthermore, we would like to express our gratitude to King Mongkut's University of Technology North Bangkok and the National Science Research and Innovation, Ministry of Higher Education, Science, and Research for supporting the research fund.

Funding

This research was funded by the National Science, Research and Innovation Fund (NSRF) and King Mongkut's University of Technology North Bangkok (Project No. KMUTNB-FF-69-B-08).

Conflict of interest

The authors declare that they have no conflicts of interest.

References

1. D. C. Montgomery, *Introduction to statistical quality control*, 8 Eds., Wiley, 2013.
2. M. Frisén, Evaluations of methods for statistical surveillance, *Stat. Med.*, **11** (1992), 1489–1502. https://doi.org/10.1002/sim.4780111107
3. R. R. Sitter, L. P. Hanrahan, D. Demets, H. A. Anderson, A monitoring system to detect increased rates of cancer incidence, *Am. J. Epidemiolgy*, **132** (1990), 123–130. https://doi.org/10.1093/oxfordjournals.aje.a115773
4. B. Mason, J. Antony, Statistical process control: An essential ingredient for improving service and manufacturing quality, *Manag. Ser. Qual.: An Int. J.*, **10** (2000), 233–238. https://doi.org/10.1108/09604520010341618
5. M. Basseville, I. V. Nikiforov, *Detection of abrupt changes: Theory and application*, USA: Prentice-Hall, 1993. Available from: `https://dl.acm.org/doi/book/10.5555/151741`.
6. B. A. Ergashev, On a CAPM monitoring based on the EWMA procedure, *Computing in Economics and Finance 2003 from Society for Computational Economics*, 2003. Available from: `https://econpapers.repec.org/paper/scescecf3/283.htm`.
7. V. Golosnoy, W. Schmid, EWMA control charts for monitoring optimal portfolio weights, *Seq. Anal.*, **26** (2006), 195–224. https://doi.org/10.1080/07474940701247099
8. M. J. Anderson, A. A. Thompson, Multivariate control charts for ecological and environmental monitoring, *Ecol. Appl.*, **14** (2004), 1921–1935.

9. W. A. Shewhart, Economic Control of Quality of Manufactured Product, *Bell. Syst. Tech. J.*, **9** 1930, 364–389. https://doi.org/10.1002/j.1538-7305.1930.tb00373.x
10. E. S. Page, Continuous inspection schemes, *Biometrika.*, **41** (1954), 100–115. https://doi.org/10.2307/2333009
11. S. W. Roberts, Control Chart Tests Based on Geometric Moving Averages, *Technometrics*, **1** (1959), 239–250. https://doi.org/10.1080/00401706.1959.10489860
12. M. B. C. Khoo, A moving average control chart for monitoring the fraction non-conforming, *Qual. Reliab. Eng. Int.*, **20** (2004), 617–635. https://doi.org/10.1002/qre.576
13. J. M. Lucas, M. S. Succucii, Exponentially weighted moving average control schemes: Properties and enhancements, *Technometrics*, **32** (1990), 1–12. https://doi.org/10.1080/00401706.1990.10484583
14. M. B. C. Khoo, V. H. Wong, A double moving average control chart, *Commum. Stat. Simul. Comput.*, **37** (2008), 1696–1708. https://doi.org/10.1080/03610910701832459
15. V. Alevizakos, K. Chatterjee, C. Koukouvinos, A. Lappa, A double moving average control chart: Discussion, *Commun. Stat. Simul. Comput.*, **51** (2022), 6043–6057. https://doi.org/10.1080/03610918.2020.1788591
16. R. Taboran, S. Sukparungee, Y. Areepong, Mixed Moving Average-Exponentially Weighted Moving Average Control Chart for Monitoring of Parameter Change, *Proceedings of The International MultiConference of Engineers and Computer Scientists 2019*, 2019, 411–415.
17. S. Sukparungsee, Y. Areepong, R. Taboran, Exponentially weighted moving average-moving average charts for monitoring the process mean, *PLoS ONE.*, **15** (2020), e0228208. https://doi.org/10.1371/journal.pone.0228208
18. M. A. Raza, K. Iqbal, M. Aslam, T. Nawaz, S. H. Bhatti, G. M. Engmann, Mixed Exponentially Weighted Moving Average-Moving Average Control Chart with Application to Combined Cycle Power Plant, *Sustainability*, **15** (2023), 3239. https://doi.org/10.3390/su15043239
19. R. Taboran, S. Sukparungsee, On Designing of a New EWMA-DMA Control Chart for Detecting Mean Shifts and Its Application, *Thailand Stat.*, **21** (2022), 148–164.
20. M. Aslam, W. Gui, N. Khan, C. H. Jun, Double moving average–EWMA control chart for exponentially distributed quality, *Commun. Stat. Simul. Comput.*, **46** (2017), 7351–7364. https://doi.org/10.1080/03610918.2016.1236955
21. N. Saengsura, Y. Areepong, S. Sukparungsee, New Designing Mixed Double Moving Average-Cumulative Sum Control Chart for Detecting Mean Shifts with Symmetrically and Asymmetrically Distributed Observations, *Appl. Sci. Eng. Prog.*, **16** (2023), 6527. https://doi.org/10.14416/j.asep.2022.12.004
22. F. Asif, M. Noor-ul-Amin, A. Riaz, Accelerated failure time model based risk adjusted MA-EWMA control chart, *Commun. Stat. Simul. Comput.*, **53** (2024), 4821–4831. https://doi.org/10.1080/03610918.2022.2155315
23. R. W. Amin, M. R. Reynolds, B. Saad, Nonparametric quality control charts based on the sign statistic, *Commun. Stat. Theory Methods*, **24** (1995), 1597–1623. https://doi.org/10.1080/03610929508831574

24. S. F. Yang, J. S. Lin, S. W. Cheng, A new parametric EWMA sign chart, *Expert Syst. Appl.*, **38** (2011), 6239–6243. https://doi.org/10.1016/j.eswa.2010.11.044

25. S. Sheu, T. Lin, The Generally Weighted Moving Average Control Chart for Detecting Small Shifts in the Process Mean, *Qual. Eng.*, **16** (2003), 209–231. https://doi.org/10.1081/QEN-120024009

26. N. Chakraborty, S. Chakraborti, S. W. Human, N. Balakrishnan, A Generally Weighted Moving Average Signed-rank Control Chart. *Qual. Reliab. Eng. Int.*, **32** (2016), 2835–2845. https://doi.org/10.1002/qre.1968

27. M. A. Raza, F. Tariq, A. A. Zaagan, G. M. Engmann, A. M. Mahnashi, M. Z. Meetei, A nonparametric mixed exponentially weighted moving average-moving average control chart with an application to gas turbines, *PLoS ONE*, **19** (2024), e0307559. https://doi.org/10.1371/journal.pone.0307559

28. W. Sudsutad, Y. Areepong, S. Sukparungee Nonparametric mixed moving average–exponentially weighted moving average control chart with applications, *Lobachevskii J. Math.*, **46** (2025), 5293–5312.

29. M. A. Raza, A. Amin, M. Aslam, T. N. M. Irfan, F. Tariq, Nonparametric mixed exponentially weighted moving average-moving average control chart, *Sci. Rep.*, **14** (2024), 6759. https://doi.org/10.1038/s41598-024-57407-1

30. R. Taboran, S. Sukparungsee, Y. Areepong, Design of a new Tukey MA-DEWMA control chart to monitor process and its applications, *IEEE Access*, **9** (2021), 102746–102757. https://doi.org/10.1109/ACCESS.2021.3098172

31. M. K. Shanshool, S. B. Mahadik, D. G. Godase, M. B. C. Khoo, The combined Shewhart-EWMA sign charts, *Qual. Reliab. Eng. Int.*, **40** (2024), 4111–4122. https://doi.org/10.1002/qre.3625

32. T. Mahmood, M. Hyder, S. M. M. Raza, M. Moeen, M. Riaz, On moving average based location charts under modified successive sampling, *Hacettepe J. Math. Stat.*, **53** (2024), 506–523. https://doi.org/10.15672/hujms.1223709

33. K. Talordphop, Y. Areepong, S. Sukparungsee, An empirical assessment of Tukey combined extended exponentially weighted moving average control chart, *AIMS Mathematics*, **10** (2025), 3945–3960. https://doi.org/10.3934/math.2025184

34. F. F. Gan, An optimal design of EWMA control charts based on median run length, *J. Stat. Comput. Simul.*, **45** (1993), 169–184. https://doi.org/10.1080/00949659308811479

35. D. Radson., A. H. Boyd, Graphical representation of run length distributions, *Qual. Eng.*, **17** (2005), 301–308. https://doi.org/10.1081/QEN-200056484

36. D. Han, F. Tsung, A reference-free cuscore chart for dynamic mean change detection and a unified framework for charting performance comparison, *J. Am. Stat. Assoc.*, **101** (2006), 368–386. https://doi.org/10.1198/016214505000000556

37. T. Munir, X. Hu, O. Kauppila, B. Bergquist, Effect of measurement uncertainty on combined quality control charts. *Comput. Ind. Eng.*, **175** (2023), 108900. https://doi.org/10.1016/j.cie.2022.108900

38. P. Castagliola, A. Achouri, H. Taleb, G. Celeno, S. Psarakis, Monitoring the coefficient of variation using a variable sample size control chart, *Int. J. Adv. Manuf. Technol.* **80** (2015), 1561–1576. https://doi.org/10.1007/s00170-015-6985-6

39. R. Shanker, H. Fesshaye, S. Selvaraj, On modeling of lifetimes data using exponential and lindley distributions, *Biom. Biostat. Int. J.*, **2** (2015), 140–147. https://doi.org/10.15406/bbij.2015.02.00042

40. J. T. Burr, *Elementary Statistical Quality Control*, 2 Eds., New York, Boca Raton: CRC Press, 2004. https://doi.org/10.1201/b15948

A. Appendix

To analyze the expected and variance values of the MEDM–sign control chart, we must know about the expected and variance values of the MEDM control chart. In the following procedure, we will analyze the variance value of the MA_{S_t} statistic for several ranges of t.

Theorem A.1. *We have the following variance values:*

$$V(MA_{S_t}) = \begin{cases} \dfrac{n}{4t}, & t < w, \\ \dfrac{n}{4w}, & t \geq w. \end{cases} \tag{A.1}$$

Proof. For $1 \leq t \leq w-1$, we have

$$V(MA_{S_t}) = \frac{1}{t^2}\sum_{j=1}^{t} V(S_j) = \frac{n}{4t^2}(t-1+1) = \frac{n}{4t}.$$

For $t \geq w-1$, we have

$$V(MA_{S_t}) = \frac{1}{w^2}\sum_{j=t-w+1}^{t} V(S_j) = \frac{n}{4w^2}(t-t+w-1+1) = \frac{n}{4w}.$$

The proof is completed. □

Lemma A.2. *For $1 \leq j_1, j_2 \leq w-1$, we have the following relation:*

$$Cov(MA_{S_{j_1}}, MA_{S_{j_2}}) = \frac{n\min\{j_1, j_2\}}{4j_1j_2} = \frac{n\Lambda_1(j_1, j_2)}{4}. \tag{A.2}$$

Proof. For $j_1 < j_2$, we have

$$Cov(MA_{S_{j_1}}, MA_{S_{j_2}}) = Cov\left(\frac{1}{j_1}\sum_{u_1=1}^{j_1} S_{u_1}, \frac{1}{j_2}\sum_{u_2=1}^{j_2} S_{u_2}\right) = \frac{1}{j_1j_2}\sum_{u_1=1}^{j_1} V(S_{u_1}) = \frac{n}{4j_2}.$$

For $j_2 < j_1$, we have the covariance $Cov(MA_{S_{j_1}}, MA_{S_{j_2}})$ is calculated by

$$Cov(MA_{S_{j_1}}, MA_{S_{j_2}}) = Cov\left(\frac{1}{j_1}\sum_{u_1=1}^{j_1} S_{u_1}, \frac{1}{j_2}\sum_{u_2=1}^{j_2} S_{u_2}\right) = \frac{1}{j_1j_2}\sum_{u_2=1}^{j_2} V(S_{u_2}) = \frac{n}{4j_1}.$$

Thus, the relation (A.2) is achieved. □

Lemma A.3. *For $1 \le j_1 \le w-1$ and $j_2 \ge w$, we have the following relation:*

$$Cov(MA_{S_{j_1}}, MA_{S_{j_2}}) = \frac{n\max\{0, w+j_1-j_2\}}{4j_1w} = \frac{n\Lambda_2(j_1,j_2)}{4}. \tag{A.3}$$

Proof. For $1 \le j_1 \le w-1$ and $j_2 \ge w$, we have the following results:

$$Cov(MA_{S_{j_1}}, MA_{S_{j_2}}) = Cov\left(\frac{1}{j_1}\sum_{u_1=1}^{j_1} S_{u_1}, \frac{1}{w}\sum_{u_2=j_2-w+1}^{j_2} S_{u_2}\right) = \frac{1}{j_1w}Cov\left(\sum_{u_1=1}^{j_1} S_{u_1}, \sum_{u_2=j_2-w+1}^{j_2} S_{u_2}\right).$$

It should be observed that when $u_1 = u_2$, we have $Cov(S_{u_1}, S_{u_2}) = 0$.
For $j_2 - w + 1 \le j_1$, we have

$$\begin{aligned} Cov(MA_{S_{j_1}}, MA_{S_{j_2}}) &= \frac{1}{j_1w}Cov\left(\sum_{u_1=1}^{j_1} S_{u_1}, \sum_{u_2=j_2-w+1}^{j_1} S_{u_2} + \sum_{u_2=j_1+1}^{j_2} S_{u_2}\right) \\ &= \frac{1}{j_1w}\sum_{u_1=j_2-w+1}^{j_1} V(S_{u_2}) \\ &= \frac{n(w+j_1-j_2)}{4j_1w}. \end{aligned}$$

For $j_2 - w + 1 > j_1$, we have

$$Cov(MA_{S_{j_1}}, MA_{S_{j_2}}) = \frac{1}{j_1w}Cov\left(\sum_{u_1=1}^{j_1} S_{u_1}, \sum_{u_2=j_2-w+1}^{j_2} S_{u_2}\right) = 0.$$

Thus, the relation (A.3) is obtained. □

Lemma A.4. *For $j_1,\ j_2 \ge w$, we have the following relation:*

$$Cov(MA_{S_{j_1}}, MA_{S_{j_2}}) = \frac{n\max\{0, w+|j_1-j_2|\}}{4w^2} = \frac{n\Lambda_3(j_1,j_2)}{4}. \tag{A.4}$$

Proof. For $j_1,\ j_2 \ge w$, and $0 < j_2 - j_1 < w$, we have the following results:

$$\begin{aligned} Cov(MA_{S_{j_1}}, MA_{S_{j_2}}) &= Cov\left(\frac{1}{w}\sum_{u_1=j_1-w+1}^{j_1} S_{u_1}, \frac{1}{w}\sum_{u_2=j_2-w+1}^{j_2} S_{u_2}\right) \\ &= \frac{1}{w^2}Cov\left(\sum_{u_1=j_1-w+1}^{j_1} S_{u_1}, \sum_{u_2=j_2-w+1}^{j_2} S_{u_2}\right) \\ &= \frac{1}{w^2}Cov\left(\sum_{u_1=j_1-w+1}^{j_2-w} S_{u_1} + \sum_{u_1=j_2-w+1}^{j_1} S_{u_1}, \sum_{u_2=j_2-w+1}^{j_1} S_{u_2} + \sum_{u_2=j_1+1}^{j_2} S_{u_2}\right) \\ &= \frac{1}{w^2}V\left(\sum_{u_1=j_2-w+1}^{j_1} S_{u_1}\right) \end{aligned}$$

$$= \frac{n(j_1 - j_2 + w)}{4w^2}.$$

Using the same procedure, for $j_1,\ j_2 \geq w$, and $0 < j_1 - j_2 < w$, we have the following results:

$$\begin{aligned}
Cov(MA_{S_{j_1}}, MA_{S_{j_2}}) &= Cov\left(\frac{1}{w}\sum_{u_1=j_1-w+1}^{j_1} S_{u_1}, \frac{1}{w}\sum_{u_2=j_2-w+1}^{j_2} S_{u_2}\right) \\
&= \frac{1}{w^2}Cov\left(\sum_{u_1=j_1-w+1}^{j_1} S_{u_1}, \sum_{u_2=j_2-w+1}^{j_2} S_{u_2}\right) \\
&= \frac{1}{w^2}Cov\left(\sum_{u_1=j_1-w+1}^{j_2} S_{u_1} + \sum_{u_1=j_2+1}^{j_1} S_{u_1}, \sum_{u_2=j_2-w+1}^{j_1-w} S_{u_2} + \sum_{u_2=j_1-w+1}^{j_2} S_{u_2}\right) \\
&= \frac{1}{w^2}V\left(\sum_{u_2=j_1-w+1}^{j_2} S_{u_1}\right) \\
&= \frac{n(j_2 - j_1 + w)}{4w^2}.
\end{aligned}$$

For $j_1,\ j_2 \geq w$, and $j_2 - j_1 > w$, we have

$$Cov(MA_{S_{j_1}}, MA_{S_{j_2}}) = Cov\left(\frac{1}{w}\sum_{u_1=j_1-w+1}^{j_1} S_{u_1}, \frac{1}{w}\sum_{u_2=j_2-w+1}^{j_2} S_{u_2}\right) = 0.$$

In addition, for $j_1,\ j_2 \geq w$, and $j_1 - j_2 > w$, we have

$$Cov(MA_{S_{j_1}}, MA_{S_{j_2}}) = Cov\left(\frac{1}{w}\sum_{u_1=j_1-w+1}^{j_1} S_{u_1}, \frac{1}{w}\sum_{u_2=j_2-w+1}^{j_2} S_{u_2}\right) = 0.$$

Thus, the relation (A.4) is obtained. □

Theorem A.5. *For $1 \leq t < w$, we have the following variance:*

$$V(DMA_{S_t}) = \frac{n}{4t^2}\left[\sum_{j=1}^{t}\frac{1}{j} + \sum_{1\leq j_1<j_2\leq t}\frac{2}{j_2}\right].$$

Proof. For $1 \leq t < w$, we have

$$V(DMA_{S_t}) = V\left(\frac{1}{t}\sum_{j=1}^{t} MA_{S_t}\right) = \frac{1}{t^2}\left[\sum_{j=1}^{t} V(MA_{S_j}) + 2\sum_{1\leq j_1<j_2\leq t} Cov(MA_{S_{j_1}}, MA_{S_{j_2}})\right].$$

Applying Theorem A.1 and Lemma A.2, for $j_1 < j_2$, we obtain

$$V(DMA_{S_t}) = \frac{n}{4t^2}\left[\sum_{j=1}^{t}\frac{1}{j} + \sum_{1\leq j_1,j_2\leq t}\frac{2}{j_2}\right].$$

The proof is done. □

Theorem A.6. *For $w \le t < 2w-1$, we have the following variance:*

$$\begin{aligned} V(DMA_{S_t}) &= \frac{n}{4w^2}\Bigg[\sum_{j=t-w+1}^{w-1}\frac{1}{j} + 2\sum_{t-w+1\le j_1<j_2\le w-1}\Lambda_1(j_1,j_2) + \frac{t-w+1}{w} \\ &\quad +2\sum_{j_1=t-w+1}^{w-1}\sum_{j_2=w}^{t}\Lambda_2(j_1,j_2) + 2\sum_{w\le j_1<j_2\le t}\Lambda_3(j_1,j_2)\Bigg]. \end{aligned} \tag{A.5}$$

Proof. For $w \le t < 2w-1$, it follows that

$$\begin{aligned} V(DMA_{S_t}) &= V\left(\frac{1}{w}\sum_{j=t-w+1}^{t}MA_{S_j}\right) \\ &= \frac{1}{w^2}V\left(\sum_{j=t-w+1}^{w-1}MA_{S_j} + \sum_{j=w}^{t}MA_{S_j}\right) \\ &= \frac{1}{w^2}\Bigg[\sum_{j=t-w+1}^{w-1}V(MA_{S_j}) + 2\sum_{t-w+1\le j_1<j_2\le w-1}Cov(MA_{S_{j_1}},MA_{S_{j_2}}) + \sum_{j=w}^{t}V(MA_{S_j}) \\ &\quad +2\sum_{j_1=t-w+1}^{w-1}\sum_{j_2=w}^{t}Cov(MA_{S_{j_1}},MA_{S_{j_2}}) + 2\sum_{w\le j_1<j_2\le t}Cov(MA_{S_{j_1}},MA_{S_{j_2}})\Bigg]. \end{aligned}$$

Applying Theorem A.1 and Lemmas A.2–A.4, we achieve the result (A.5). □

Theorem A.7. *For $t \ge 2w-1$, we have the following variance:*

$$V(DMA_{S_t}) = \frac{n}{4w^2}\left[1 + 2\sum_{t-w+1\le j_1<j_2\le t}\Lambda_3(j_1,j_2)\right]. \tag{A.6}$$

Proof. Since $t \ge 2w-1$, we find that $t-w+1 \ge w$. We then have

$$\begin{aligned} V(DMA_{S_t}) &= V\left(\frac{1}{w}\sum_{j=t-w+1}^{t}MA_{S_j}\right) \\ &= \frac{1}{w^2}V\left(\sum_{j=t-w+1}^{t}MA_{S_j}\right) \\ &= \frac{1}{w^2}\left[\sum_{j=t-w+1}^{t}V(MA_{S_j}) + 2\sum_{t-w+1\le j_1<j_2\le t}Cov(MA_{S_{j_1}},MA_{S_{j_2}})\right]. \end{aligned}$$

Applying Theorem A.1 and Lemma A.4, we achieve the result (A.5). □

From all results in Theorems A.5–A.7, the following conclusion can be given:

$$V(DMA_{S_t}) = \begin{cases} \dfrac{n}{4t^2}\left[\displaystyle\sum_{j=1}^{t}\frac{1}{j} + \sum_{j_1=1}^{t-1}\sum_{j_2=j_1+1}^{t}\frac{2}{j_2}\right], & 1 \le t < w, \\ \dfrac{n}{4w^2}\Bigg[\displaystyle\sum_{j_1=t-w+1}^{w-1}\frac{1}{j_1} + \sum_{t-w+1\le j_1<j_2\le w-1}\frac{2}{j_2} + \frac{t-w+1}{w} \\ \quad + \displaystyle\sum_{j_1=t-w+1}^{w-1}\sum_{j_2=w}^{t} 2\Lambda_2(j_1,j_2) + \sum_{w\le j_1<j_2\le t} 2\Lambda_3(j_1,j_2)\Bigg], & w \le t < 2w-1, \\ \dfrac{n}{4w^2}\left[1 + \displaystyle\sum_{t-w+1\le j_1<j_2\le t} 2\Lambda_3(j_1,j_2)\right], & t \ge 2w-1. \end{cases} \tag{A.7}$$

Lemma A.8. *For $1 \le j_1, j_2 \le w-1$, we have the following relation:*

$$Cov(DMA_{S_{j_1}}, DMA_{S_{j_2}}) = \frac{n}{4j_1j_2}\sum_{u_1=1}^{j_1}\sum_{u_2=1}^{j_2}\Lambda_1(u_1,u_2). \tag{A.8}$$

Proof. For $1 \le j_1, j_2 \le w-1$, it follows that

$$Cov(DMA_{S_{j_1}}, DMA_{S_{j_2}}) = Cov\left(\frac{1}{j_1}\sum_{u_1=1}^{j_1}MA_{S_{u_1}}, \frac{1}{j_2}\sum_{u_2=1}^{j_2}MA_{S_{u_2}}\right) = \frac{1}{j_1j_2}\sum_{u_1=1}^{j_1}\sum_{u_2=1}^{j_2}Cov(MA_{S_{u_1}}, MA_{S_{u_2}}).$$

Applying Lemma A.2, we obtain the relation (A.8). □

Lemma A.9. *For $1 \le j_1 \le w-1$ and $w \le j_2 < 2w-1$, we have the following relation:*

$$Cov(DMA_{S_{j_1}}, DMA_{S_{j_2}}) = \frac{n}{4j_1w}\left[\sum_{u_1=1}^{j_1}\sum_{u_2=j_2-w+1}^{w-1}\Lambda_1(u_1,u_2) + \sum_{u_1=1}^{j_1}\sum_{u_2=w}^{j_2}\Lambda_2(u_1,u_2)\right]. \tag{A.9}$$

Proof. For $1 \le j_1 \le w-1$ and $w \le j_2 < 2w-1$, we find that

$$\begin{aligned} Cov(DMA_{S_{j_1}}, DMA_{S_{j_2}}) &= Cov\left(\frac{1}{j_1}\sum_{u_1=1}^{j_1}MA_{S_{u_1}}, \frac{1}{w}\sum_{u_2=j_2-w+1}^{j_2}MA_{S_{u_2}}\right) \\ &= \frac{1}{j_1w}\left(\sum_{u_1=1}^{j_1}\sum_{u_2=j_2-w+1}^{w-1}Cov(MA_{S_{u_1}}, MA_{S_{u_2}}) + \sum_{u_1=1}^{j_1}\sum_{u_2=w}^{j_2}Cov(MA_{S_{u_1}}, MA_{S_{u_2}})\right). \end{aligned}$$

Applying Lemma A.2 and Lemma A.3, the relation (A.9) is achieved. □

Lemma A.10. *For $1 \le j_1 \le w-1$ and $j_2 \ge 2w-1$, we have the following relation:*

$$Cov(DMA_{S_{j_1}}, DMA_{S_{j_2}}) = \frac{n}{4j_1w}\sum_{u_1=1}^{j_1}\sum_{u_2=j_2-w+1}^{w-1}\Lambda_2(u_1,u_2). \tag{A.10}$$

Proof. For $1 \le j_1 \le w-1$ and $j_2 \ge 2w-1$, we obtain

$$Cov(DMA_{S_{j_1}}, DMA_{S_{j_2}}) = Cov\left(\frac{1}{j_1}\sum_{u_1=1}^{j_1} MA_{S_{u_1}}, \frac{1}{w}\sum_{u_2=j_2-w+1}^{j_2} MA_{S_{u_2}}\right) = \frac{1}{j_1 w}\sum_{u_1=1}^{j_1}\sum_{u_2=j_2-w+1}^{j_2} Cov(MA_{S_{u_1}}, MA_{S_{u_2}}).$$

Applying Lemma A.3, the relation (A.10) is achieved. □

Lemma A.11. *For $w \le j_1, j_2 < 2w-1$, we have the following relation:*

$$\begin{aligned} Cov(DMA_{S_{j_1}}, DMA_{S_{j_2}}) &= \frac{n}{4w^2}\Bigg[\sum_{u_1=j_1-w+1}^{w-1}\sum_{u_2=j_2-w+1}^{w-1}\Lambda_1(u_1,u_2) + \sum_{u_1=j_1-w+1}^{w-1}\sum_{u_2=w}^{j_2}\Lambda_2(u_1,u_2) \\ &\quad + \sum_{u_1=w}^{j_1}\sum_{u_2=j_2-w+1}^{w-1}\Lambda_2(u_1,u_2) + \sum_{u_1=w}^{j_1}\sum_{u_2=w}^{j_2}\Lambda_3(u_1,u_2)\Bigg]. \end{aligned} \tag{A.11}$$

Proof. For $w \le j_1, j_2 < 2w-1$, it follows that

$$\begin{aligned} Cov(DMA_{S_{j_1}}, DMA_{S_{j_2}}) &= Cov\left(\frac{1}{w}\sum_{u_1=j_1-w+1}^{j_1} MA_{S_{u_1}}, \frac{1}{w}\sum_{u_2=j_2-w+1}^{j_2} MA_{S_{u_2}}\right) \\ &= \frac{1}{w^2}\Bigg[\sum_{u_1=j_1-w+1}^{w-1}\sum_{u_2=j_2-w+1}^{w-1} Cov(MA_{S_{u_1}}, MA_{S_{u_2}}) + \sum_{u_1=j_1-w+1}^{w-1}\sum_{u_2=w}^{j_2} Cov(MA_{S_{u_1}}, MA_{S_{u_2}}) \\ &\quad + \sum_{u_1=w}^{j_1}\sum_{u_2=j_2-w+1}^{w-1} Cov(MA_{S_{u_1}}, MA_{S_{u_2}}) + \sum_{u_1=w}^{j_1}\sum_{u_2=w}^{j_2} Cov(MA_{S_{u_1}}, MA_{S_{u_2}})\Bigg]. \end{aligned}$$

Applying Lemmas A.2–A.4, the relation (A.11) is obtained. □

Lemma A.12. *For $w \le j_1 < 2w-1$ and $j_2 \ge 2w-1$, we have the following relation:*

$$Cov(DMA_{S_{j_1}}, DMA_{S_{j_2}}) = \frac{n}{4w^2}\left[\sum_{u_1=j_1-w+1}^{w-1}\sum_{u_2=j_2-w+1}^{j_2}\Lambda_2(u_1,u_2) + \sum_{u_1=w}^{j_1}\sum_{u_2=j_2-w+1}^{j_2}\Lambda_3(u_1,u_2)\right]. \tag{A.12}$$

Proof. For $w \le j_1 < 2w-1$ and $j_2 \ge 2w-1$, we have

$$\begin{aligned} Cov(DMA_{S_{j_1}}, DMA_{S_{j_2}}) &= Cov\left(\frac{1}{w}\sum_{u_1=j_1-w+1}^{j_1} MA_{S_{u_1}}, \frac{1}{w}\sum_{u_2=j_2-w+1}^{j_2} MA_{S_{u_2}}\right) \\ &= \frac{1}{w^2}\left[\sum_{u_1=j_1-w+1}^{w-1}\sum_{u_2=j_2-w+1}^{j_2} Cov(MA_{S_{u_1}}, MA_{S_{u_2}}) + \sum_{u_1=w}^{j_1}\sum_{u_2=j_2-w+1}^{j_2} Cov(MA_{S_{u_1}}, MA_{S_{u_2}})\right]. \end{aligned}$$

Applying Lemma A.3 and Lemma A.4, the relation (A.12) is achieved. □

Lemma A.13. *For $j_1, j_2 \ge 2w-1$, we have the following relation:*

$$Cov(DMA_{S_{j_1}}, DMA_{S_{j_2}}) = \frac{n}{4w^2}\sum_{u_1=j_1-w+1}^{j_1}\sum_{u_2=j_2-w+1}^{j_2}\Lambda_3(u_1,u_2). \tag{A.13}$$

Proof. For $j_1,\ j_2 \geq 2w-1$, we get

$$\begin{aligned} Cov(DMA_{S_{j_1}}, DMA_{S_{j_2}}) &= Cov\left(\frac{1}{w}\sum_{u_1=j_1-w+1}^{j_1} MA_{S_{u_1}}, \frac{1}{w}\sum_{u_2=j_2-w+1}^{j_2} MA_{S_{u_2}}\right) \\ &= \frac{1}{w^2}\sum_{u_1=j_1-w+1}^{j_1}\sum_{u_2=j_2-w+1}^{j_2} Cov(MA_{S_{u_1}}, MA_{S_{u_2}}). \end{aligned}$$

Applying Lemma A.4, the relation (A.12) is obtained. □

From all results in Lemmas A.8–A.13, the following conclusion can be drawn:

$$Cov(DMA_{S_{j_1}}, DMA_{S_{j_2}}) = \begin{cases} \dfrac{n}{4j_1j_2}\left[\displaystyle\sum_{u_1=1}^{j_1}\frac{1}{u_1} + \sum_{1\leq u_1<u_2\leq j_1}\frac{2}{u_2} + \sum_{u_1=1}^{j_1}\sum_{u_2=u_1+1}^{j_2}\frac{1}{u_2}\right], \\ \qquad 1 \leq j_1, j_2 \leq w-1, \\ \dfrac{n}{4j_1w}\left[\displaystyle\sum_{u_1=1}^{j_1}\sum_{u_2=j_2-w+1}^{w-1}\Lambda_1(u_1,u_2) + \sum_{u_1=1}^{j_1}\sum_{u_2=w}^{j_2}\Lambda_2(u_1,u_2)\right], \\ \qquad w \leq t < 2w-1,\ t-w+1 \leq j_1 \leq w-1,\ w \leq j_2 \leq t, \\ \dfrac{n}{4j_1w}\left[\displaystyle\sum_{u_1=j_1-w+1}^{j_2-w}\sum_{u_2=j_2-w+1}^{w-1}\Lambda_1(u_1,u_2) + \sum_{u_1=j_1-w+1}^{j_2-w}\sum_{u_2=w}^{j_2}\Lambda_2(u_1,u_2)\right. \\ \quad + \displaystyle\sum_{u_1=j_2-w+1}^{w-1}\frac{1}{u_1} + \frac{j_1-w+1}{w} + \sum_{j_2-w+1\leq u_1<u_2\leq w-1}\frac{2}{u_2} \\ \quad + \displaystyle\sum_{u_1=j_2-w+1}^{w-1}\sum_{u_2=w}^{j_1}2\Lambda_2(u_1,u_2) + \sum_{w\leq u_1<u_2\leq j_1}2\Lambda_3(u_1,u_2) \\ \quad \left. + \displaystyle\sum_{u_1=j_2-w+1}^{w-1}\sum_{u_2=j_1+1}^{j_2}\Lambda_3(u_1,u_2) + \sum_{u_1=w}^{j_1}\sum_{u_2=j_1+1}^{j_2}\Lambda_3(u_1,u_2)\right], \\ \qquad w \leq j_1 < j_2 < 2w-1, \\ \dfrac{n}{4w^2}\left[\displaystyle\sum_{u_1=j_1-w+1}^{w-1}\sum_{u_2=j_2-w+1}^{j_2}\Lambda_2(u_1,u_2) + \sum_{u_1=w}^{j_1}\sum_{u_2=j_2-w+1}^{j_2}\Lambda_3(u_1,u_2)\right] \\ \qquad w \leq j_1 \leq 2w-2,\ 2w-1 \leq j_2 \leq 3w-3, \\ \dfrac{n}{4w^2}\displaystyle\sum_{u_1=j_1-w+1}^{j_1}\sum_{u_2=j_2-w+1}^{j_2}\Lambda_3(u_1,u_2), w \leq u_1 < 2w-1, u_2 \geq 2w-1. \end{cases} \tag{A.14}$$